

Comparison of dark energy models using late-universe observations

Peng-Ju Wu^{1,*}

¹*School of Physics, Ningxia University, Yinchuan 750021, China*

In the framework of general relativity, dark energy was proposed to explain the cosmic acceleration. A pivotal inquiry in cosmology is to determine whether dark energy is the cosmological constant, and if not, the challenge lies in constraining how it evolves with time. In this paper, we utilize the latest observational data to constrain some typical dark energy models, and make a comparison for them according to their capabilities of fitting the current data. Our study is confined to late-universe observations, including the baryon acoustic oscillation, type Ia supernova, cosmic chronometer, and strong gravitational lensing time delay data. We employ the Akaike information criterion (AIC), deviance information criterion (DIC), and Bayesian information criterion (BIC) to assess the worth of models. The AIC and DIC analyses indicate that all dark energy models outperform the Λ CDM model. However, the BIC analysis leaves room for Λ CDM due to its heavier penalty on the model complexity. Compared to Λ CDM, most dark energy models are robustly supported by AIC and DIC while being explicitly disfavored by BIC. The models that are robustly favored by AIC and DIC and not explicitly disfavored by BIC include the w CDM, interacting dark energy, and Ricci dark energy models. Furthermore, we observe that an alternative modified gravity model exhibits superior performance when compared with Λ CDM across all information criteria.

I. INTRODUCTION

It is generally believed that cosmic acceleration originates from the so-called dark energy, which has negative pressure and accounts for approximately 70% of the energy budget of the universe. The investigation into the nature of dark energy has become one of the most important issues in the field of fundamental physics. In the standard model of cosmology, dark energy is considered as the cosmological constant Λ , which is associated to the zero-point vacuum energy density of quantum fields. The Λ cold dark matter (Λ CDM) model has shown excellent agreement with various observations over an extended period [1]. However, it faces some theoretical challenges [2, 3]. Recently, it has also encountered several measurement inconsistencies, particularly regarding the Hubble constant¹ H_0 , cosmic curvature parameter² Ω_K , and the amplitude of the matter power spectrum³ σ_8 [24–31]. All of these issues have driven researchers to seek underestimated systematic errors or new physics beyond the standard model.

Cosmologists have conceived many physically-rich dark energy models to address the difficulties encountered by the standard model. For instance, a slowly rolling scalar field can also generate negative pressure, thereby driving the current phase of cosmic acceleration. Such light scalar fields provide a potential mechanism for dynamical

dark energy [32–39]. Generally, one can characterize the properties of dark energy through parametrizing its equation of state (EoS) as $w = p_{\text{de}}/\rho_{\text{de}}$, where p_{de} and ρ_{de} represent the pressure and energy density of dark energy, respectively. The simplest parametrized model, where w is a constant, is commonly referred to as the w CDM model [40]. This model subsumes two distinct scenarios of dark energy: Quintessence, which corresponds to cases where $w > -1$ [37], and Phantom, which pertains to instances where $w < -1$. A more physical and realistic scenario is that w varies with cosmic time, and one of the most common parametrizations is $w = w_0 + w_a(1 - a)$ [41, 42], where a is the cosmic scale factor. For more dark energy EoS parametrizations, see Refs. [43–47].

A variety of extensions to the Λ CDM model and scalar field theories are worth investigating, such as taking into account the spatial geometry of the universe or the interaction between dark energy and dark matter. On the one hand, some studies indicate that our universe may not be spatially flat. For example, the cosmic microwave background (CMB) observations favor a closed universe [48, 49], while the combination of non-CMB probes supports an open universe [31]. While the two results exhibit a statistical discrepancy, both imply a non-flat universe. It should be stressed that the dark energy EoS and Ω_K are degenerate. Thus, it is necessary to incorporate Ω_K into parameter space and examine its impact on the dark energy EoS measurement. On the other hand, there may be an interaction between dark energy and dark matter. From the view of particle physics, interactions are ubiquitous. Cosmologists suggest that dark energy may have a non-gravitational interaction with dark matter, which is described by the interacting dark energy (IDE) models [50–55]. According to some recent studies, there is evidence suggesting the presence of interaction between dark sectors; however, the conclusion is contingent upon the underlying IDE models [56–62].

Some dark energy models are built upon deep theoret-

* wupengju@nxu.edu.cn

¹ It should be noted that the Hubble tension primarily arises between Cepheid-SNIa distance ladders and CMB analysis; however, many other low-redshift H_0 measurements are consistent with the CMB value, see Refs. [4–16].

² There are also some studies argue against the existence of a curvature tension, see Refs. [17–20].

³ There is probably no longer a σ_8 measurement inconsistency, at least the main one between weak lensing and CMB observations has been resolved, see Refs. [21–23].

ical considerations. For example, the holographic dark energy (HDE) model is posited to have a quantum gravity origin. It is constructed by incorporating gravitational effects into the effective quantum field theory via the holographic principle, which proposes that the number of degrees of freedom in a spatial region is finite to prevent the black hole formation [63, 64]. The model not only presents a unique perspective on the nature of dark energy but also demonstrates the potential to resolve the puzzles faced by the standard model. Its theoretical variant, the Ricci dark energy (RDE) model [65], has also garnered a lot of attention. The distinction between HDE and RDE hinges on the selection of the infrared cutoff utilized in the computation of dark energy density. Specifically, HDE opts for the radius of the future event horizon of the universe as the infrared cutoff, while RDE employs the average radius of the Ricci scalar curvature as the infrared cutoff. Investigating these two models is crucial for exploring quantum gravity-based explanations of dark energy [66–71].

In physics, there are actually two mechanisms that can account for the accelerated expansion of the universe, i.e., assuming the existence of dark energy or modifying the gravity on large scales. The latter is termed modified gravity (MG) theory, which can produce “effective dark energy” scenarios mimicking the behavior of actual dark energy. By setting aside the issues of structure growth, it is possible to consider such models as alternatives to dark energy models. A prominent exemplar of such theoretical constructs is the Dvali-Gabadze-Porrati (DGP) model [72]. This model originates within the framework of braneworld theories, which propose that our observable universe is a brane embedded in a higher-dimensional space, known as the “bulk”. In the DGP model, gravity exhibits a tendency to leak into the bulk at cosmological scales, which contributes to the observed acceleration of our universe. The theoretical variant of DGP, the α DM model [73], has also been widely studied due to its ability to better fit the historical observational data.

Facing numerous rival dark energy models, the primary objective is to determine which one represents the true dark energy scenario. However, achieving this is exceedingly challenging. A more practical goal is to discern which ones can better fit the observational data. [74]. Currently, there exist some measurement discrepancies between the early- and late-universe observations. For instance, the H_0 value measured by the Cepheid-supernova distance ladder is in above 5σ tension with that derived from the CMB observations assuming Λ CDM [25]. When integrating observations to constrain cosmological parameters, it is necessary to consider the potential measurement inconsistencies among different datasets. The existence of these tensions diminish the justifiability of combining CMB with late-universe probes for param-

eter inference⁴ The motivation of this work is to constrain various dark energy models using the combination of late-universe observations and assess the worth of them.

We consider four non-CMB probes, including the baryon acoustic oscillation (BAO, standard ruler), type Ia supernova (SN, standard candle), cosmic chronometer (CC, standard clock), and strong gravitational lensing time delay (TD) observations. For an extended period, these non-CMB observations failed to effectively constrain dark energy models. However, recent advancements may have altered this situation. Recently, the DESI collaboration released the high-precision BAO data [30, 75–77], the DES program published the high-quality samples of SN Ia [78], and to date, there are 32 CC data [79] and 7 TD data [80–88] have become available for parameter estimation. We shall employ these late-universe observational data to constrain dark energy models.

The paper is organized as follows: Sec. II outlines the methodology, Sec. III details the observational data and their processing procedures, Sec. IV compares different dark energy models, and Sec. V concludes with key findings and their cosmological implications.

II. METHODOLOGY

The constraints on cosmological parameters stem from precise measurements of cosmological distances; we start with a review of the definitions and distinctions between key distance metrics in cosmology. Firstly, the comoving distance is defined as

$$D_C(z) = \int_0^z \frac{cdz'}{H(z')} = \frac{c}{H_0} \int_0^z \frac{dz'}{E(z')}, \quad (1)$$

where $E(z) = H(z)/H_0$ is the reduced Hubble parameter. The transverse comoving distance is given by [89]

$$D_M(z) = \begin{cases} \frac{c}{H_0\sqrt{\Omega_K}} \sinh \left[\frac{H_0\sqrt{\Omega_K}}{c} D_C(z) \right] & \text{if } \Omega_K > 0, \\ D_C(z) & \text{if } \Omega_K = 0, \\ \frac{c}{H_0\sqrt{-\Omega_K}} \sin \left[\frac{H_0\sqrt{-\Omega_K}}{c} D_C(z) \right] & \text{if } \Omega_K < 0. \end{cases} \quad (2)$$

Then the luminosity distance, angular diameter distance, and Hubble distance can be written as

$$D_L = D_M(1+z); \quad D_A = D_M/(1+z); \quad D_H = c/H. \quad (3)$$

The measurement of these cosmological distances enables the imposition of constraints on parameters embedded in

⁴ It should be stressed that although discrepancies exist between early- and late-time data, this does not imply that all observations between early- and late universe are inconsistent. Additionally, inconsistencies may also exist among the various late-universe cosmological probes themselves.

the $E(z)$ formalism, and the primary distinctions among different cosmological models are reflected in the form of $E(z)$.

In this work, we adopt the Markov Chain Monte Carlo (MCMC) analysis to infer the probability distributions of cosmological parameters using the observational data, by maximizing the likelihood $L \propto \exp(-\chi^2/2)$. The χ^2 function of each dataset can be written as $\Delta\mathbf{D}^T\mathbf{C}^{-1}\Delta\mathbf{D}$, where $\Delta\mathbf{D}$ is the vector of observable residuals representing the difference between observation and theory, and \mathbf{C} is the covariance matrix. We measure the convergence of the chains by checking that all parameters have $R - 1 < 0.01$, where R is the potential scale reduction factor of the Gelman-Rubin diagnostics. We shall make a comparison for different dark energy models according to their capabilities of fitting the current data.

As models become more complex (i.e., have more free parameters), they tend to fit the observational data better, which can lead to a lower χ^2 value. Therefore, the χ^2 comparison is unfair for comparing dark energy models. In this work, we adopt the Akaike information criterion (AIC), Bayesian information criterion (BIC), and deviance information criterion (DIC) to compare different models. AIC is defined as

$$\text{AIC} = \chi_{\min}^2 + 2k, \quad (4)$$

where k is the number of free parameters. A model with a smaller AIC is more favored by observations. BIC is calculated by

$$\text{BIC} = \chi_{\min}^2 + k \ln N, \quad (5)$$

where N is the number of data points used in the fitting. DIC is calculated by

$$\text{DIC} = \chi_{\min}^2 + 2k_{\text{eff}}, \quad (6)$$

where $k_{\text{eff}} = \langle \chi^2 \rangle - \chi_{\min}^2$ is the the number of effectively constrained parameters. Here, the angular brackets denote the average over the posterior distribution.

In practice, we are not concerned with the absolute values of A/B/DIC, but the relative value between different models, i.e., $\Delta\text{A/B/DIC}$. In this work, the flat Λ CDM model is adopted as the reference. Negative $\Delta\text{A/B/DIC}$ values denote superior fit to the observational data relative to flat Λ CDM, whereas positive values indicate inferior fit. Generally, a negative $\Delta\text{A/B/DIC}$ value within the range $[-2, 0)$ indicates weak evidence in favor of the model, a value within $[-6, -2)$ indicates positive evidence in favor, a value within $[-10, -6)$ indicates strong evidence in favor, and a value less than -10 indicates very strong evidence in favor. Conversely, a $\Delta\text{A/B/DIC}$ value within the range $(0, 2]$ indicates weak evidence against the model, a value within $(2, 6]$ indicates positive evidence against, a value within $(6, 10]$ indicates strong evidence against, and a value greater than 10 indicates very strong evidence against. The penalty terms of AIC and DIC depend exclusively on the number of parameters, not

TABLE I. The BAO measurements from DESI. Here, r_d is the sound horizon at the drag epoch and $D_V(z)$ is the comoving volume-averaged distance which is calculated by $[D_M(z)]^{2/3} [cD_H(z)]^{1/3}$.

Redshift z	Observable	Value
0.30	D_V/r_d	7.93 ± 0.15
0.51	D_M/r_d	13.62 ± 0.25
0.51	D_H/r_d	20.98 ± 0.61
0.71	D_M/r_d	0.497 ± 0.045
0.71	D_H/r_d	13.38 ± 0.18
0.93	D_M/r_d	22.43 ± 0.48
0.93	D_H/r_d	0.459 ± 0.038
1.32	D_M/r_d	17.65 ± 0.30
1.32	D_H/r_d	19.78 ± 0.46
1.49	D_V/r_d	0.473 ± 0.041
2.33	D_M/r_d	19.5 ± 1.0
2.33	D_H/r_d	19.6 ± 2.1

sample size. Therefore, once the number of data points is large, the results may favor the model with more parameters. To further penalize the model complexity, BIC takes into account the number of data points. Using AIC, BIC, and DIC together gives a complete picture when comparing models.

III. OBSERVATIONAL DATA

• **Baryon Acoustic Oscillations.** We consider the recently released DESI BAO data and summarize them in Table I. The data points with same redshifts are correlated, and the covariance matrices can be found in the website.⁵ Note that the sound horizon at the drag epoch is treated as a free parameter in the MCMC analysis, which can ensure that the derived constraints are independent of the early-universe observational priors.

• **Type Ia Supernovae.** We consider the DES sample of 1829 distant SNe Ia spanning $0.025 < z < 1.3$ [78]. Compared to the PantheonPlus sample, the dataset quintuples the number of SNe beyond $z > 0.5$. The distance modulus for an SN Ia is defined by $\mu = m_B - M_B$, where m_B is the observed apparent magnitude in the rest-frame B -band, and M_B denotes the absolute magnitude. The theoretical distance modulus is calculated by

$$\mu_{\text{th}}(z) = 5 \log \left[\frac{D_L(z)}{\text{Mpc}} \right] + 25. \quad (7)$$

The observational data, encompassing distance moduli, their associated uncertainties and covariance between distinct data points, are accessible on the website.⁶

• **Cosmic Chronometers.** The CC method provides a direct way to measure the Hubble parameter. We summarize the latest 32 CC $H(z)$ measurements in Table II.

⁵ <https://data.desi.lbl.gov/doc/releases/>

⁶ <https://github.com/des-science/DES-SN5YR>

TABLE II. The 32 $H(z)$ measurements obtained with the CC method.

Redshift z	$H(z)$ [km/s/Mpc]	Reference
0.07	69 ± 19.6	[90]
0.09	69 ± 12	[91]
0.12	68.6 ± 26.2	[90]
0.17	83 ± 8	[91]
0.179	75 ± 4	[92]
0.199	75 ± 5	[92]
0.2	72.9 ± 29.6	[90]
0.27	77 ± 14	[91]
0.28	88.8 ± 36.6	[90]
0.352	83 ± 14	[92]
0.38	83 ± 13.5	[93]
0.4	95 ± 17	[91]
0.4004	77 ± 10.2	[93]
0.425	87.1 ± 11.2	[93]
0.445	92.8 ± 12.9	[93]
0.47	89 ± 49.6	[94]
0.4783	80.9 ± 9	[93]
0.48	97 ± 62	[95]
0.593	104 ± 13	[92]
0.68	92 ± 8	[92]
0.75	98.8 ± 33.6	[96]
0.781	105 ± 12	[92]
0.875	125 ± 17	[92]
0.88	90 ± 40	[95]
0.9	117 ± 23	[91]
1.037	154 ± 20	[92]
1.3	168 ± 17	[91]
1.363	160 ± 33.6	[97]
1.43	177 ± 18	[91]
1.53	140 ± 14	[91]
1.75	202 ± 40	[91]
1.965	186.5 ± 50.4	[97]

Among them, 15 data points from Refs. [92, 93, 97] are correlated, and the covariance matrix can be found in the website⁷.

• **Strong Gravitational Lensing.** We consider the existing seven SGL systems with time-delay distance and angular diameter distance measurements, and summarize them in Table III. The time-delay distance is defined by

$$D_{\Delta t} \equiv (1 + z_l) \frac{D_l D_s}{D_{ls}}, \quad (8)$$

where D_l , D_s , and D_{ls} are the angular diameter distances between observer and lens, between observer and source, and between lens and source, respectively. Note that the errors of data will be approximated to a Gaussian form. For more details, we refer readers to the website.⁸

TABLE III. The time-delay distances and angular diameter distances for TD measurements. Here, z_l and z_s are the redshifts of lens and source respectively.

z_l	z_s	$D_{\Delta t}$ [Mpc]	D_l [Mpc]	References
0.6304	1.394	5156^{+296}_{-236}	1228^{+177}_{-151}	[80, 81]
0.295	0.654	2096^{+98}_{-83}	804^{+141}_{-112}	[82, 83]
0.4546	1.693	2707^{+183}_{-168}	—	[83, 84]
0.745	1.789	5769^{+589}_{-471}	1805^{+555}_{-398}	[85]
0.6575	1.662	4784^{+399}_{-248}	—	[86]
0.311	1.722	1470^{+137}_{-127}	697^{+186}_{-144}	[83]
0.597	2.375	3382^{+146}_{-115}	1711^{+376}_{-280}	[87, 88]

IV. DARK ENERGY MODELS

In this section, we describe the dark energy models selected for analysis and report the constraint results from the combination of late-universe observations. We utilize the same datasets to constrain these models and conduct a comparison for them. For organizational purposes, we divide these models into six distinct groups:

- (a) Cosmological constant model.
- (b) Dark energy models with a parameterized EoS.
- (c) Dark energy models assuming a non-flat universe.
- (d) Interacting dark energy models.
- (e) Holographic dark energy models.
- (f) Effective dark energy models (MG theories).

The constraint results for dark energy models are shown in Table IV. The results of the model comparison using the information criteria are summarized in Table V. The posterior distribution contours are shown in Figs. 1–12, with no statistically significant discrepancies among late-universe datasets observed.

A. Cosmological constant model

The cosmological constant Λ , corresponding to the energy density of quantum vacuum fluctuations, has become the leading explanation for dark energy since the discovery of cosmic acceleration in 1998. Despite facing some theoretical challenges [2, 3], it aligns well with various historical observations [1]. The Λ CDM model, which incorporates Λ and cold dark matter to describe the cosmic composition and expansion, is considered as the standard model of cosmology. The equation of state for Λ is -1 , and the reduced Hubble parameter for Λ CDM is given by

$$E(z) = [\Omega_m(1+z)^3 + (1 - \Omega_m)]^{1/2}, \quad (9)$$

where Ω_m is the matter density parameter. Note that the contribution from radiation is overlooked throughout the

⁷ <https://gitlab.com/mmoresco/CCcovariance>

⁸ <https://zenodo.org/records/3633035>

TABLE IV. Fit results for the dark energy models by using the observational data. Here H_0 is in units of km/s/Mpc.

Model	Parameter			
Λ CDM	$H_0 = 72.7^{+1.2}_{-1.2}$	$\Omega_m = 0.317^{+0.011}_{-0.011}$		
DGP	$H_0 = 71.5^{+1.2}_{-1.2}$	$\Omega_m = 0.245^{+0.010}_{-0.010}$		
$\text{o}\Lambda$ CDM	$H_0 = 72.8^{+1.1}_{-1.3}$	$\Omega_m = 0.286^{+0.019}_{-0.019}$	$\Omega_K = 0.106^{+0.056}_{-0.056}$	
$\text{l}\Lambda$ CDM	$H_0 = 71.9^{+1.3}_{-1.3}$	$\Omega_m = 0.380^{+0.027}_{-0.027}$	$\beta = -0.36^{+0.14}_{-0.14}$	
α DE	$H_0 = 72.1^{+1.3}_{-1.3}$	$\Omega_m = 0.284^{+0.022}_{-0.017}$	$\alpha = 0.56^{+0.22}_{-0.22}$	
HDE	$H_0 = 71.8^{+1.3}_{-1.3}$	$\Omega_m = 0.266^{+0.014}_{-0.014}$	$c = 1.112^{+0.093}_{-0.120}$	
RDE	$H_0 = 71.8^{+1.2}_{-1.2}$	$\Omega_m = 0.212^{+0.012}_{-0.012}$	$\gamma = 0.554^{+0.019}_{-0.022}$	
w CDM	$H_0 = 71.9^{+1.2}_{-1.2}$	$\Omega_m = 0.295^{+0.014}_{-0.014}$	$w = -0.877^{+0.046}_{-0.046}$	
$\text{l}w$ CDM	$H_0 = 71.9^{+1.2}_{-1.4}$	$\Omega_m = 0.53^{+0.31}_{-0.14}$	$w = -1.72^{+1.10}_{-0.45}$	$\beta = -2.5^{+3.3}_{-1.3}$
ow CDM	$H_0 = 72.0^{+1.3}_{-1.3}$	$\Omega_m = 0.289^{+0.019}_{-0.019}$	$w = -0.890^{+0.065}_{-0.050}$	$\Omega_K = 0.023^{+0.073}_{-0.073}$
CPL	$H_0 = 71.0^{+1.3}_{-1.3}$	$\Omega_m = 0.329^{+0.018}_{-0.015}$	$w_0 = -0.725^{+0.084}_{-0.097}$	$w_a = -1.32^{+0.65}_{-0.65}$
JBP	$H_0 = 70.9^{+1.3}_{-1.3}$	$\Omega_m = 0.324^{+0.017}_{-0.016}$	$w_0 = -0.64^{+0.11}_{-0.12}$	$w_a = -2.23^{+1.1}_{-0.97}$

TABLE V. Summary of the information criteria results.

Model	χ^2_{\min}	ΔAIC	ΔBIC	ΔDIC
Λ CDM	1686.282	0	0	0
DGP	1684.453	-1.829	-1.829	-1.798
$\text{o}\Lambda$ CDM	1682.493	-1.789	3.752	-1.814
$\text{l}\Lambda$ CDM	1679.213	-5.069	0.472	-4.710
α DE	1680.915	-3.367	2.175	-3.547
HDE	1680.787	-3.495	2.046	-3.399
RDE	1679.183	-5.092	0.442	-5.069
w CDM	1679.190	-5.092	0.449	-4.972
$\text{l}w$ CDM	1679.181	-3.101	7.982	-4.644
ow CDM	1679.119	-3.163	7.920	-2.873
CPL	1674.821	-7.461	3.622	-7.389
JBP	1674.480	-7.802	3.281	-8.024

paper, because its influence becomes negligible compared to matter and dark energy in the late-time universe.

Using the observational data, we can obtain the best-fit values for cosmological parameters and the corresponding χ^2 value as follows:

$$\Omega_m = 0.317, H_0 = 72.7 \text{ km/s/Mpc}, \chi^2_{\min} = 1686.282.$$

We present the $1\sigma - 2\sigma$ posterior distribution contours for the Λ CDM model in Fig. 1. As can be seen, the matter density parameter Ω_m is consistent with the Planck CMB result, but the H_0 value is in around 4.1σ tension with that derived from the CMB observations [1]. We note that measurement inconsistencies exist among

late-universe observations themselves. For example, the BAO data provide $\Omega_m = 0.295^{+0.014}_{-0.015}$, while the SN data give $\Omega_m = 0.352 \pm 0.017$; there is a 2.5σ tension between the two results. While these values suggest a degree of inconsistency, it is below the commonly accepted 3σ threshold for significant tension. Hence, it is considered appropriate to combine these datasets. Among all the models selected for analysis, Λ CDM is noted for having the highest χ^2_{\min} . However, this does not indicate the poorest fit to the observational data. Generally, models with a greater number of parameters tend to have a lower χ^2_{\min} due to their increased flexibility in accommodating data. Considering its simplicity and sustained favorable performance in cosmological research, we choose the flat Λ CDM model as the reference for analyzing and comparing other models.

B. Dark energy models with parameterized EoS

In this category, we explore three dark energy models with parameterized EoS: the constant w (w CDM) model, the Chevallier–Polarski–Linder (CPL) model, and the Jassal–Bagla–Padmanabhan (JBP) model.

1. Constant w parametrization

In the w CDM model, the dark energy EoS is described by a constant w . The value of w can be any real number, allowing for dark energy to have dynamical properties. For instance, if $w < -1$, the energy density of dark energy increase as the universe expands. The growth in energy density engenders a repulsive force that not only continues to accelerate the cosmic expansion but does so at an ever-increasing rate. This scenario could potentially lead

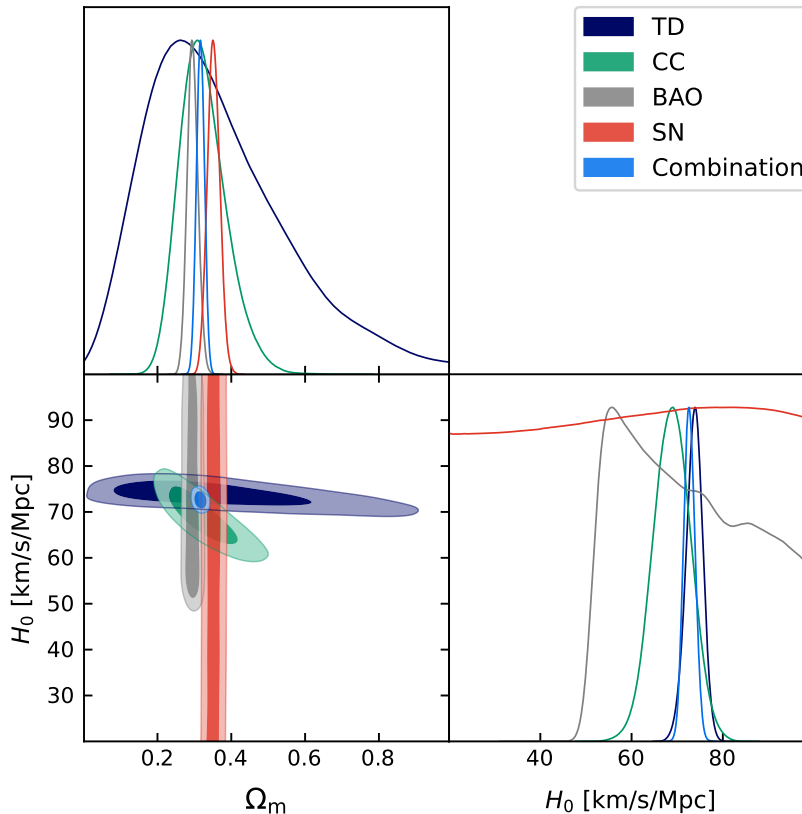


FIG. 1. The cosmological constant model: 68.3% and 95.4% confidence contours derived from individual TD, CC, BAO, and SN datasets, and their combined analysis (TD+CC+BAO+SN).

to the Big Rip, where the expansion rate is so rapid that it overcomes the gravitational forces that bind matter together, resulting in the disintegration of all structures in the universe. In contrast, when $w > -1$, the energy density of dark energy decreases as the universe expands. If $-1 < w < -1/3$, the universe sustains a gradually weakening acceleration. For cases where $w \geq -1/3$, the universe reverts to the decelerated expansion, and in closed universe models, may ultimately lead to contraction in future epochs. The w CDM model introduces an additional degree of freedom compared to Λ CDM, which allows for more flexible fitting to the observational data. For this model, the reduced Hubble parameter is given by

$$E(z) = \left[\Omega_m (1+z)^3 + (1 - \Omega_m)(1+z)^{3(1+w)} \right]^{1/2}. \quad (10)$$

Using the observational data, we can get the best-fit parameters and the corresponding χ^2 as follows:

$$\begin{aligned} \Omega_m &= 0.295, \quad H_0 = 71.9 \text{ km/s/Mpc}, \quad w = -0.877, \\ \chi_{\min}^2 &= 1679.190. \end{aligned}$$

The $1\sigma - 2\sigma$ posterior distribution contours for w CDM are shown in Fig. 2. As can be seen, the central value of w is situated within the quintessence-like regime,

where $w > -1$. Furthermore, the cosmological constant scenario is excluded at approximately 2σ confidence level. Our results are consistent with the constraints reported in Refs. [30, 77, 78]. Comprehensive analyses of w CDM using earlier observational data can be found in Refs. [19, 40]. Compared to the flat Λ CDM model, the w CDM model yields $\Delta\text{AIC} = -5.092$, $\Delta\text{DIC} = -4.972$ and $\Delta\text{BIC} = 0.449$. Negative ΔAIC and ΔDIC values indicate that the model provides an improved fit to the observational data relative to the flat Λ CDM, with values between -6 and -2 constituting positive evidence for this improvement. A positive ΔBIC value suggests an inferior fit to current data relative to the flat Λ CDM. However, since $\Delta\text{BIC} < 2$, the evidence against the w CDM model is only weak.

2. The Chevallier–Polarski–Linder parametrization

The w CDM model serves as a foundational construct for exploring the dynamics of dark energy. However, the assumption of a constant EoS may not fully capture the complexity of dark energy's behavior [98–102]. This has motivated the introduction of more intricate models such as the CPL model [41, 42]. It parameterizes the dark energy EoS as a linear function of the scale factor a ,

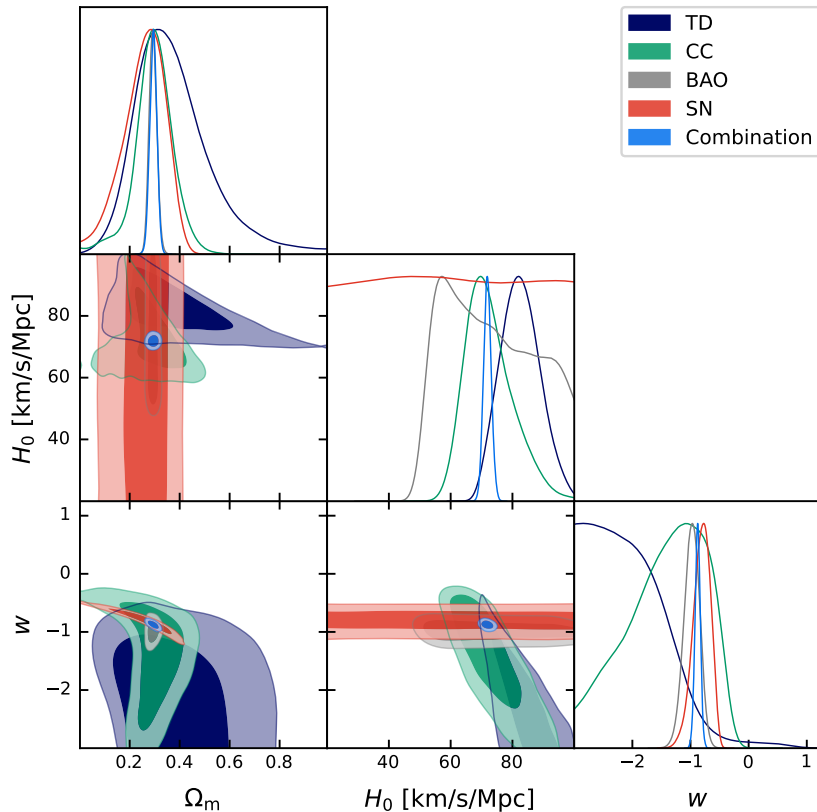


FIG. 2. The constant w model: 68.3% and 95.4% confidence contours derived from individual TD, CC, BAO, and SN datasets, and their combined analysis (TD+CC+BAO+SN).

given by $w(z) = w_0 + w_a(1 - a)$, where w_0 and w_a are free parameters. For this model, we have

$$E(z) = [\Omega_m(1+z)^3 + (1 - \Omega_m)(1+z)^{3(1+w_0+w_a)} \exp\left(-\frac{3w_a z}{1+z}\right)]^{1/2}. \quad (11)$$

Through the joint observational data analysis, we can obtain the best-fit parameters and the corresponding χ^2 as:

$$\Omega_m = 0.329, \quad H_0 = 71.0 \text{ km/s/Mpc}, \quad w_0 = -0.725, \\ w_a = -1.32, \quad \chi_{\min}^2 = 1674.821.$$

The $1\sigma - 2\sigma$ likelihood contours for the CPL model are shown in Fig. 3. As can be seen, the constraint results are not consistent with the Λ CDM model, i.e., the point ($w_0 = -1$ and $w_a = 0$) does not fall within the 1σ region. The cosmological constant is excluded at almost 3σ confidence level. The joint data favor the region with $w_0 > -1$ and $w_a < 0$, implying that EoS was phantom-like in the distant past and has evolved to quintessence-like at present. Our results are consistent with the recent studies, see Refs. [30, 77, 78]. Note that pre-DESI analyses likewise indicated a statistical preference for dynamical dark energy [103, 104]. The CPL model yields

a ΔAIC value of -7.461 and a ΔDIC value of -7.389 when compared to the flat Λ CDM, providing strong evidence for an improved fit to the data. Both AIC and DIC penalize the CPL model for the number of model parameters, whereas BIC further penalizes the model for both the number of parameters and the sample size, leading to $\Delta\text{BIC} = 3.622$. The BIC result suggests that the observational data provide a support for the flat Λ CDM model over the CPL model, with $2 < \Delta\text{BIC} < 6$ constituting positive evidence. The discrepancies in the outcomes of AIC/DIC and BIC primarily stem from their distinct evaluative strategies.

3. The Jassal-Bagla-Padmanabhan parametrization

The JBP model was proposed to solve the high- z issues inherent in the CPL model [45]. It parameterizes the dark energy EoS as $w(z) = w_0 + w_a z / (1+z)^2$, where w_0 and w_a are also free parameters. In this model, the reduced Hubble parameter is calculated by

$$E(z) = [\Omega_m(1+z)^3 + (1 - \Omega_m)(1+z)^{3(1+w_0)} \exp\left(\frac{3w_a z^2}{2(1+z)^2}\right)]^{1/2}. \quad (12)$$

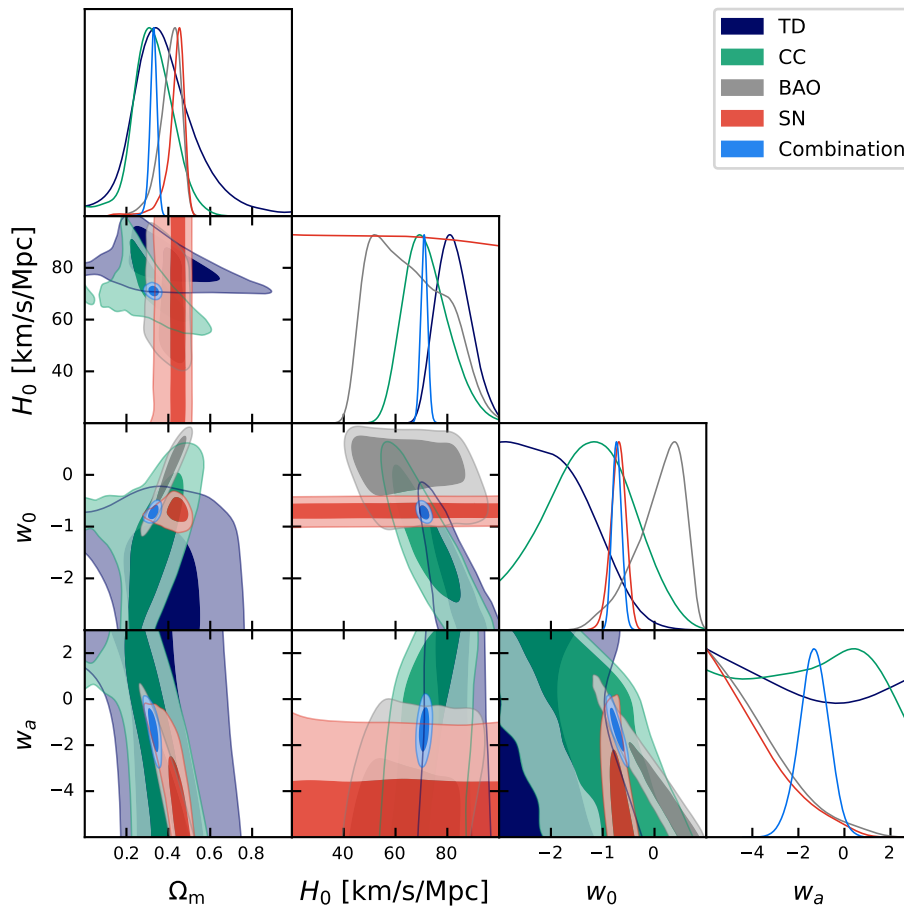


FIG. 3. The Chevallier–Polarski–Linder model: 68.3% and 95.4% confidence contours derived from individual TD, CC, BAO, and SN datasets, and their combined analysis (TD+CC+BAO+SN).

Based on the observational data, the best-fit parameters and the corresponding χ^2 are:

$$\begin{aligned} \Omega_m &= 0.324, \quad H_0 = 70.9 \text{ km/s/Mpc}, \quad w_0 = -0.64, \\ w_a &= -2.23, \quad \chi^2_{\min} = 1674.480. \end{aligned}$$

The $1\sigma - 2\sigma$ likelihood contours for the JBP model are shown in Fig. 4. We find that the constraint results are still inconsistent with the Λ CDM model. The best-fit EoS parameters for this model exhibit a greater deviation from the cosmological constant scenario than those of the CPL model. The combined analysis favors the parameter space with $w_0 > -1$ and $w_a < 0$. This solution exhibits tension with the previous study based on earlier BAO, SN and quasars [105], which reported a preference for $w_0 < -1$ and $w_a > 0$. Moreover, Ref. [106] reports $w_0 = -1.02 \pm 0.04$ and $w_a = 0.22 \pm 0.23$ using the combination of early- and late-universe observations, consistent with the Λ CDM model. The JBP model yields the most negative ΔAIC (-7.802) and ΔDIC (-8.024) values, indicating that it is most favored by the observational data (with strong evidence). However, from the perspective of BIC, the difference between this model and Λ CDM

reaches 3.281, which implies that the current data favor the Λ CDM model over JBP (with positive evidence). The dynamical dark energy models, CPL and JBP, show similar performance, both strongly supported by AIC and DIC but significantly opposed by BIC.

C. Dark energy models assuming a non-flat universe.

In this group, we explore two cosmological models: the Λ CDM model assuming a non-flat universe, denoted as $o\Lambda$ CDM, and the w CDM model assuming a non-flat universe, referred to as ow CDM.

1. Λ CDM assuming a non-flat universe

Recent studies suggest that our universe may not be spatially flat. For instance, the CMB observations tend to favor a closed universe [1, 48, 49], while the late-time observations support an open universe [31]. Although these two measurements are inconsistent and even

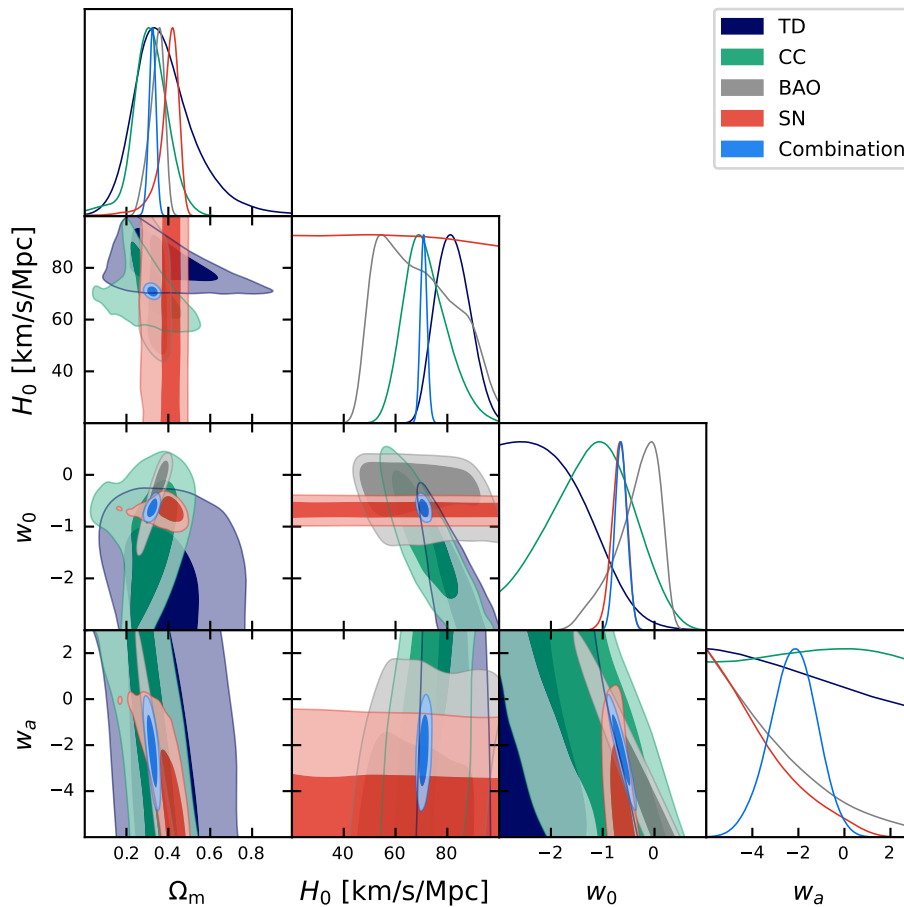


FIG. 4. The Jassal–Bagla–Padmanabhan model: 68.3% and 95.4% confidence contours derived from individual TD, CC, BAO, and SN datasets, and their combined analysis (TD+CC+BAO+SN).

contradictory, they both support the concept of a non-Euclidean universe. A non-zero curvature would have far-reaching consequences for the inflationary paradigm and the ultimate fate of the universe. Therefore, incorporating the cosmic curvature into the parameter space is imperative when constraining cosmological parameters. For the $\text{o}\Lambda\text{CDM}$ model, we have

$$E(z) = [\Omega_m(1+z)^3 + \Omega_K(1+z)^2 + (1 - \Omega_m - \Omega_K)]^{1/2}. \quad (13)$$

By using the observational data, we can obtain the best-fit parameters and the corresponding χ^2 as follows:

$$\begin{aligned} \Omega_m &= 0.286, \quad H_0 = 72.8 \text{ km/s/Mpc}, \quad \Omega_K = 0.106, \\ \chi_{\text{min}}^2 &= 1682.493. \end{aligned}$$

We present the 1σ – 2σ posterior distribution contours for the $\text{o}\Lambda\text{CDM}$ model in Fig. 5. As shown in the $\Omega_m - \Omega_K$ plane, the data combination favors an open universe, specially $\Omega_K = 0.106 \pm 0.056$, which is in around 2.6σ tension with the Planck CMB result that our universe is closed, i.e., $\Omega_K = -0.044^{+0.018}_{-0.015}$. The two measurements have opposite signs, suggesting they are contrary to each other.

Note that when the CC data is excluded, the derived constraints demonstrate increased statistical preference for an open universe, as highlighted in Ref. [31]. It should be stressed that there are also some studies argue against the existence of a curvature tension, see Refs. [17–20]. Compared to the ΛCDM model, the $\text{o}\Lambda\text{CDM}$ model yields $\Delta\text{AIC} = -1.789$, $\Delta\text{DIC} = -1.814$ and $\Delta\text{BIC} = 3.752$. Both the AIC and DIC analyses demonstrate a statistical preference for the non-flat ΛCDM model over the flat one (with weak evidence), while the BIC analysis provides positive evidence supporting the flat ΛCDM model as a more favorable model over the non-flat one.

2. $w\text{CDM}$ assuming a non-flat universe

It should be stressed that there is a strong degeneracy between the dark energy EoS and cosmic curvature. The current observational data leave room for deviations of the curvature parameter from zero (see Sec. IV C 1), which undermines the persuasiveness of the dark energy EoS constraints under the assumption of the flat uni-

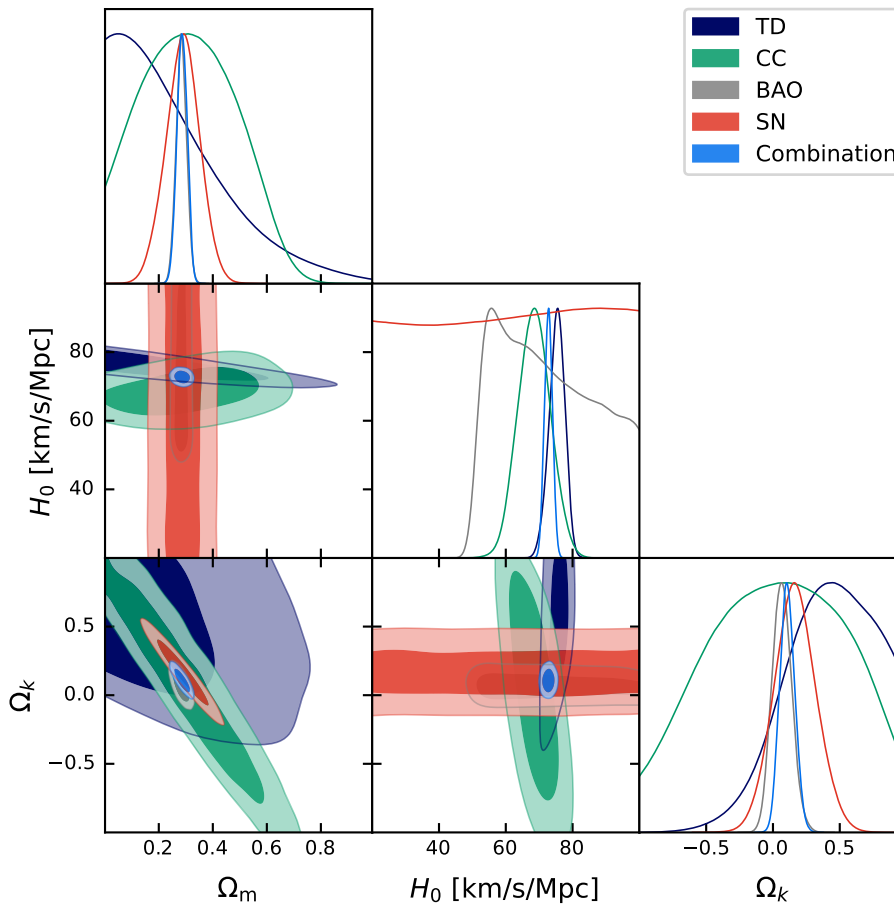


FIG. 5. The non-flat Λ CDM model: 68.3% and 95.4% confidence contours derived from individual TD, CC, BAO, and SN datasets, and their combined analysis (TD+CC+BAO+SN).

verse scenario. Therefore, it is imperative to consider the spatial curvature parameter in the dynamic dark energy constraints. Here, we select the non-flat w CDM model to conduct our analysis. In this model, the reduced Hubble parameter can be written as

$$E(z) = \left[\Omega_m(1+z)^3 + \Omega_K(1+z)^2 + (1 - \Omega_m - \Omega_K)(1+z)^{3(1+w)} \right]^{1/2}. \quad (14)$$

According to the sampling results, the optimal parameter estimates and the corresponding χ^2 value are:

$$\Omega_m = 0.289, \quad H_0 = 72.0 \text{ km/s/Mpc}, \quad w = -0.890, \\ \Omega_K = 0.023, \quad \chi^2_{\min} = 1679.119.$$

The $1\sigma - 2\sigma$ posterior distribution contours for ow CDM are shown in Fig. 6. As can be seen, the constraint result is consistent with the spatially flat universe, specially $\Omega_K = 0.023 \pm 0.073$. However, the central value of Ω_K is positive and has a significant deviation from zero. The flat universe can be ruled out at $> 1\sigma$ confidence level even in the w CDM model by excluding the

CC data, as discussed in Ref. [31]. However, the authors pointed out that their constraints are dominated by the DESI BAO data, and the results require further verification with DESI's upcoming full-shape power spectrum. We also find that the central value of EoS parameter lies within the quintessence-like regime ($w > -1$), and the cosmological constant falls out the 2σ region. Our previous analysis revealed that the w CDM model is favored by AIC/DIC and not significantly opposed by BIC (see Sec. IV B 1). The ow CDM model has an additional parameter compared to w CDM and it yields a lower χ^2_{\min} , but the difference is very small, specially $\Delta\chi^2_{\min} = -0.071$. The ow CDM model produces a Δ AIC value of -3.163 and a Δ DIC value of -2.873 when compared to the flat Λ CDM, suggesting that it provides a better fit to the observational data (with positive evidence). BIC further penalizes the model with sample size, leading to Δ BIC = 7.920, which suggests that the current data provide a substantial support for the flat Λ CDM model over the ow CDM model, with a strong evidence (Δ BIC > 6).

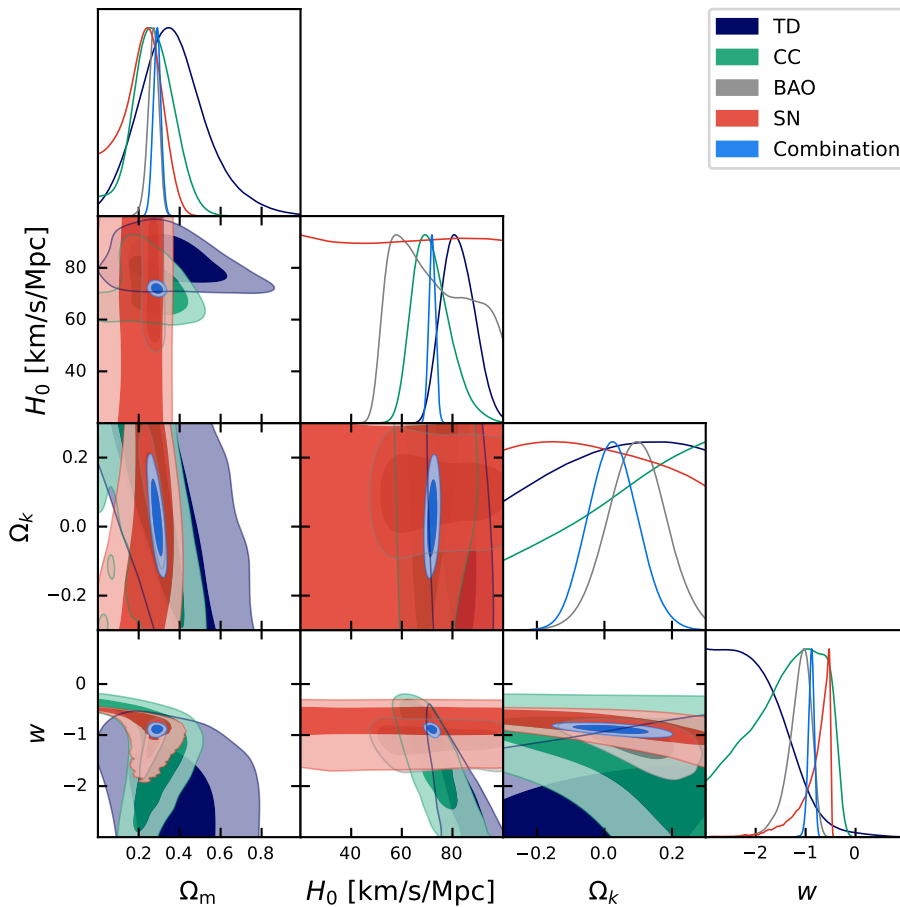


FIG. 6. The non-flat w CDM model: 68.3% and 95.4% confidence contours derived from individual TD, CC, BAO, and SN datasets, and their combined analysis (TD+CC+BAO+SN).

D. Interacting dark energy models

The interacting dark energy models offer an extension to the standard model by introducing a dynamic interaction between dark energy and dark matter, potentially resolving theoretical cosmological issues and providing a more consistent picture with the observational data [50–55, 58, 59]. If there exists an interaction between dark sectors, the energy conservation equations can be written as

$$\begin{aligned}\dot{\rho}_{\text{de}} &= -3H(1+w)\rho_{\text{de}} + Q, \\ \dot{\rho}_{\text{c}} &= -3H\rho_{\text{c}} - Q,\end{aligned}\quad (15)$$

where ρ_{de} and ρ_{c} are the energy densities of dark energy and dark matter, respectively, the dot denotes the derivative with respect to time, w is the dark energy EoS, and Q is the energy transfer rate. In this paper, we employ a phenomenological form of $Q = \beta H\rho_{\text{de}}$, where β is a dimensionless coupling parameter; $\beta > 0$ indicates that dark matter decays into dark energy, $\beta < 0$ denotes that dark energy decays into dark matter, and $\beta = 0$ means that there is no interaction between them.

1. Λ CDM with an interaction between dark sectors

In the context of the standard model, if we consider an interaction between dark energy and cold dark matter, the reduced Hubble parameter can be written as

$$\begin{aligned}E(z) &= [\Omega_{\text{m}}(1+z)^3 \\ &+ (1-\Omega_{\text{m}}) \left(\frac{\beta}{\beta+3}(1+z)^3 + \frac{3}{\beta+3}(1+z)^{-\beta} \right)]^{1/2}.\end{aligned}\quad (16)$$

For simplicity, we refer to this model as I Λ CDM.

By using the joint data, we can obtain the best-fit cosmological parameters and the corresponding χ^2 as:

$$\begin{aligned}\Omega_{\text{m}} &= 0.380, \quad H_0 = 71.9 \text{ km/s/Mpc}, \quad \beta = -0.36, \\ \chi_{\text{min}}^2 &= 1679.213.\end{aligned}$$

We present the $1\sigma - 2\sigma$ posterior distribution contours for the I Λ CDM model in Fig. 7. It can be seen that the observational data support the existence of an interaction between dark sectors at a confidence level exceeding 2σ ,

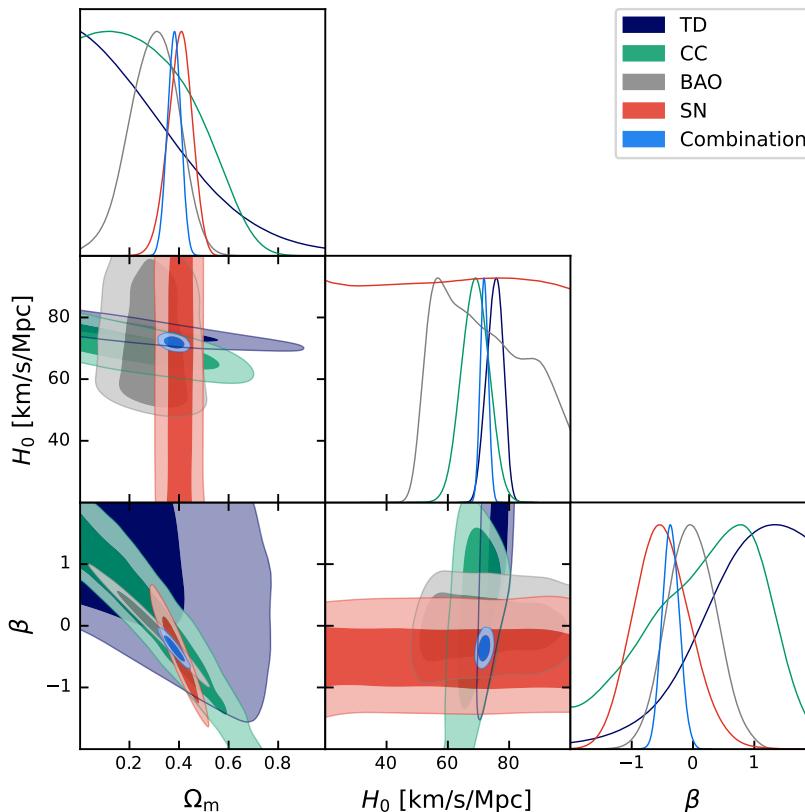


FIG. 7. The Λ CDM model with an interaction between dark energy and dark matter: 68.3% and 95.4% confidence contours derived from individual TD, CC, BAO, and SN datasets, and their combined analysis (TD+CC+BAO+SN).

with the conversion of dark energy into dark matter. This finding aligns with several recent studies; see Refs. [58–61] for details. It is crucial to emphasize that, given the unknown nature of dark matter and dark energy, the consideration of interactions rely on assumed forms. Consequently, the existence of such interactions is inherently contingent upon the specific form assumed [56–61]. For this model, we have $\Delta\text{AIC} = -5.069$, $\Delta\text{DIC} = -4.710$, and $\Delta\text{BIC} = 0.472$. Negative ΔAIC and ΔDIC values indicate that the model provides a substantial improvement fit to the observations than Λ CDM (with positive evidence). A positive ΔBIC suggests Λ CDM is preferred over $\text{I}\Lambda\text{CDM}$, but a ΔBIC value less 2 is considered weak evidence against $\text{I}\Lambda\text{CDM}$.

2. w CDM with an interaction between dark sectors

Considering that dark energy may not be the cosmological constant, it becomes imperative to extend investigations to dynamical dark energy models. If we consider an interaction between dark matter and dark energy in the w CDM model, the dimensionless Hubble parameter

can be written as

$$E(z) = \left[\Omega_m(1+z)^3 + (1-\Omega_m) \left(\frac{\beta}{\beta-3w}(1+z)^3 + \frac{3w}{3w-\beta}(1+z)^{(3+3w-\beta)} \right) \right]^{1/2}. \quad (17)$$

For simplicity, we refer to this model as $\text{I}w\text{CDM}$.

By using the observational data, the best-fit cosmological parameters and the corresponding χ^2 are:

$$\begin{aligned} \Omega_m &= 0.53, \quad H_0 = 71.9 \text{ km/s/Mpc}, \quad w = -1.72 \\ \beta &= -2.5, \quad \chi_{\min}^2 = 1679.181. \end{aligned}$$

The 1σ – 2σ likelihood contours for the $\text{I}w\text{CDM}$ model are shown in Fig. 8. As can be seen, there is a strong degeneracy between the dark energy EoS parameter w and the coupling parameter β , which impedes robust constraints on both of them. The constraint result is consistent with the Λ CDM model, i.e., the point ($w = -1$ and $\beta = 0$) falls within the 1σ region. Interestingly, by allowing for interaction, the $\text{I}w\text{CDM}$ model shifts the central value of dark energy EoS from quintessence (see Sec. IV B 1) to phantom. The $\text{I}w\text{CDM}$ model has an additional parameter compared to the $w\text{CDM}$ model and it yields a lower χ_{\min}^2 , but the difference is very small $\Delta\chi_{\min}^2 = -0.009$.

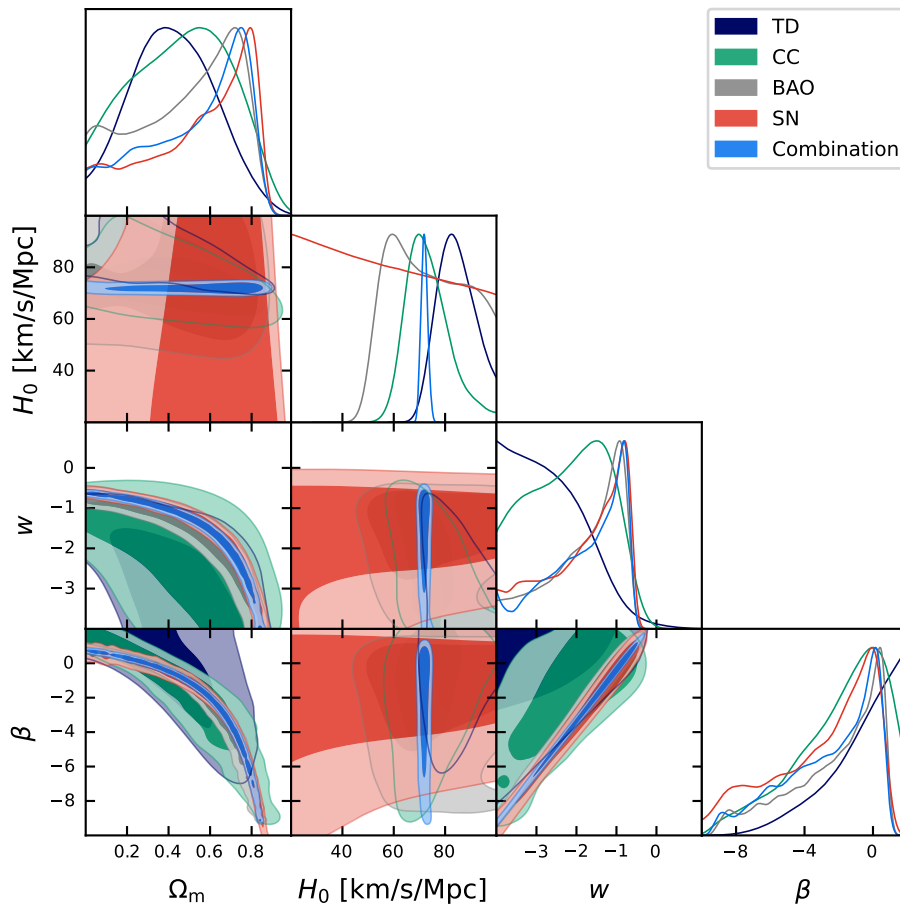


FIG. 8. The w CDM model with an interaction between dark energy and dark matter: 68.3% and 95.4% confidence contours derived from individual TD, CC, BAO, and SN datasets, and their combined analysis (TD+CC+BAO+SN).

The Iw CDM model produces a ΔAIC value of -3.101 and a ΔDIC value of -4.644 when compared to Λ CDM, indicating positive evidence for an improved fit to the observational data. BIC further penalizes the model with sample size, yielding $\Delta\text{BIC} = 7.920$, which indicates strong evidence against the Iw CDM model ($\Delta\text{BIC} > 6$).

E. Holographic dark energy models

In quantum field theory, the calculated vacuum energy density diverges. Even with the implementation of a reasonable ultraviolet (UV) cutoff, the calculated vacuum energy density remains approximately 120 orders of magnitude greater than the observed value. This discrepancy arises from the absence of a complete and coherent theory of quantum gravity. The HDE model was proposed in this context, which integrates gravitational effects into the effective quantum field theory via the holographic principle [63, 64]. This principle posits that the number of degrees of freedom in a spatial region is finite to prevent black hole formation, which would otherwise occur with an excessive number of degrees. In the HDE model,

the density of dark energy is determined by

$$\rho_{\text{de}} \propto M_{\text{pl}}^2 L^{-2}, \quad (18)$$

where M_{pl} is the reduced Planck mass and L is the infrared (IR) cutoff length scale in the effective quantum field theory. Consequently, the UV divergence issue encountered in the computation of vacuum energy density is effectively recast as an IR issue. The implementation of different IR cutoff prescriptions would result in varied cosmological consequences. This study employs two widely adopted computational methodologies for the IR cutoff.

1. Holographic dark energy model

The HDE model is formulated by employing the cosmic event horizon radius as the IR cutoff within holographic principle framework [64]. In this model, the density of dark energy is given by

$$\rho_{\text{de}} = 3c^2 M_{\text{pl}}^2 R_{\text{h}}^{-2}, \quad (19)$$

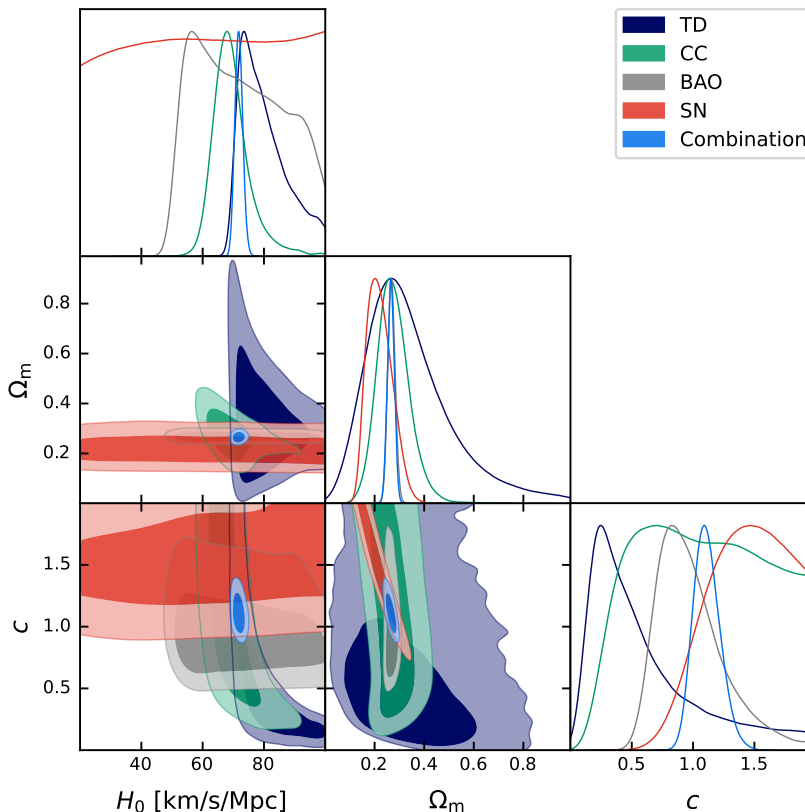


FIG. 9. The holographic dark energy model: 68.3% and 95.4% confidence contours derived from individual TD, CC, BAO, and SN datasets, and their combined analysis (TD+CC+BAO+SN).

where c is a dimensionless parameter that influences the characteristics of HDE and R_h is the future event horizon, calculated by

$$R_h(a) = a \int_a^\infty \frac{da'}{H(a')a'^2}. \quad (20)$$

The dynamical evolution of dark energy is governed by the following differential equations

$$\frac{1}{E(z)} \frac{dE(z)}{dz} = -\frac{\Omega_{de}(z)}{1+z} \left(\frac{1}{2} + \frac{\sqrt{\Omega_{de}(z)}}{c} - \frac{3}{2\Omega_{de}(z)} \right), \quad (21)$$

$$\frac{d\Omega_{de}(z)}{dz} = -\frac{2\Omega_{de}(z)(1-\Omega_{de}(z))}{1+z} \times \left(\frac{1}{2} + \frac{\sqrt{\Omega_{de}(z)}}{c} \right), \quad (22)$$

where $\Omega_{de}(z)$ is the fractional density of dark energy.

From the joint data analysis, we can get the best-fit parameters and the corresponding χ^2 as:

$$\Omega_m = 0.266, \quad H_0 = 71.8 \text{ km/s/Mpc}, \quad c = 1.112$$

$$\chi_{\min}^2 = 1680.787.$$

We plot the likelihood contours for the HDE model in Fig. 9. Unlike the Λ CDM model, the EoS for the HDE

model is dynamically evolving. The parameter c is pivotal in determining the behavior of the dark energy EoS. When $c > 1$, the EoS of HDE remains above -1 , with HDE exhibiting quintessence-like behavior. In contrast, for $c < 1$, the EoS of HDE may cross the phantom divide at $w = -1$ in the future, leading to a universe dominated by phantom-like dark energy, which is predicted to end in a catastrophic Big Rip. As can be seen, the data combination shows a preference for $c > 1$, indicating a quintessence-like behavior for HDE, and the universe is expected to undergo a relatively stable evolution. Our findings align with the latest HDE research [66–68]. Nevertheless, several critical discussions are warranted: Current late-universe observations favor $c > 1$, whereas early-universe observations support $c < 1$. This apparent inconsistency suggests two possible interpretations — either the HDE framework fails to accurately describe the cosmological evolution, or undetected systematic errors exist in measurements. We plan to conduct an investigation of this issue in future works. The HDE model yields $\Delta\text{AIC} = -3.495$, $\Delta\text{DIC} = -3.399$ and $\Delta\text{BIC} = 2.046$. As can be seen, while AIC and DIC metrics provide positive evidence favoring the HDE model, BIC provides comparable evidence against HDE due to its heavier penalty on the model complexity.

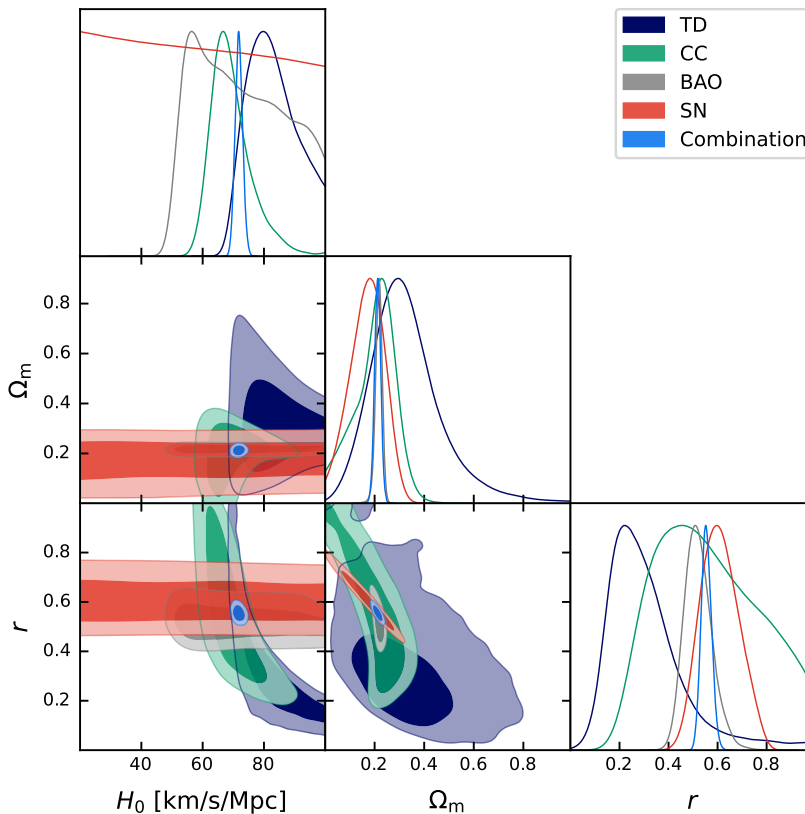


FIG. 10. The Ricci dark energy model: 68.3% and 95.4% confidence contours derived from individual TD, CC, BAO, and SN datasets, and their combined analysis (TD+CC+BAO+SN).

2. Ricci dark energy model

The RDE model proposes that the dark energy density is proportional to the Ricci scalar, which is a measure of the curvature of spacetime [65]. Unlike the HDE model, which is based on the entropy bound of quantum systems, RDE is rooted in the geometry of spacetime itself. This makes RDE an attractive model for further exploration, as it may offer insights into the interplay between quantum mechanics and general relativity, which is crucial for understanding the universe at its fundamental level. The RDE model chooses the mean radius of the Ricci scalar curvature as the IR cutoff length scale, and the dark energy density is given by

$$\rho_{\text{de}} = 3\gamma M_{\text{pl}}^2 (\dot{H} + 2H^2), \quad (23)$$

where γ is a positive constant. The evolution of the Hubble parameter is determined by the following differential equation,

$$E^2 = \Omega_m e^{-3x} + \gamma \left(\frac{1}{2} \frac{dE^2}{dx} + 2E^2 \right), \quad (24)$$

where $x \equiv \ln a$. Solving this equation, we obtain

$$E(z) = \left(\frac{2\Omega_m}{2-\gamma} (1+z)^3 + \left(1 - \frac{2\Omega_m}{2-\gamma} \right) (1+z)^{(4-\frac{2}{\gamma})} \right)^{1/2}. \quad (25)$$

Using the observational data, we can derive the best-fit values for cosmological parameters and the corresponding χ^2 as follows:

$$\begin{aligned} \Omega_m &= 0.212, \quad H_0 = 71.8 \text{ km/s/Mpc}, \quad \gamma = 0.554 \\ \chi_{\text{min}}^2 &= 1679.183. \end{aligned}$$

The $1\sigma - 2\sigma$ likelihood contours for the RDE model are shown in Fig. 10. The RDE model is capable of avoiding the causality problem faced by the HDE model, and it can also naturally resolve the coincidence problem. The parameter γ plays a crucial role in determining the behavior of dark energy. For example, during the dark energy-dominated epoch, $\gamma > 0.5$ leads to $w > -1$, while $\gamma < 0.5$ would result in $w < -1$. As can be seen, the data combination shows a preference for $\gamma > 0.5$, indicating a quintessence-like behavior for RDE. Ref. [67] establishes joint early- and late-universe constraints on the RDE model, with strong evidence indicating $\gamma < 0.5$. This discrepancy may stem from early-time observations

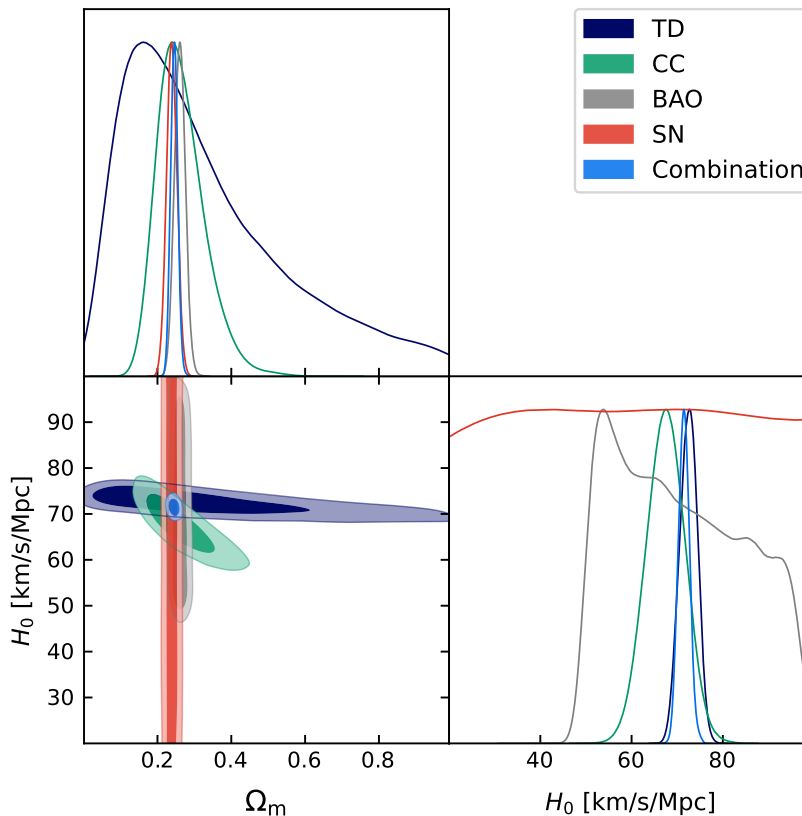


FIG. 11. The Dvali–Gabadadze–Porrati model: 68.3% and 95.4% confidence contours derived from individual TD, CC, BAO, and SN datasets, and their combined analysis (TD+CC+BAO+SN).

tending to favor $\gamma < 0.5$. A previous study, utilizing the observational data available at the time (inclusive of the CMB data), robustly ruled out the RDE model [74]. However, the data we utilized here provide a contrary conclusion. Compared to the Λ CDM model, the RDE model yields $\Delta\text{AIC} = -5.092$, $\Delta\text{DIC} = -5.069$ and $\Delta\text{BIC} = 0.442$. Negative ΔAIC and ΔDIC values indicate that the RDE model offers a better fit to the current data (with positive evidence) compared to the Λ CDM model. A positive ΔBIC value suggests a preference for the Λ CDM model over the RDE model, but only with weak evidence ($\Delta\text{BIC} < 2$). Therefore, the RDE model demonstrates commendable performance and warrants further exploration and attention.

F. Effective dark energy models (MG theories)

In physics, the observed acceleration of the universe is commonly attributed to one of two possibilities: the presence of dark energy or the deviations from Einstein’s general relativity on cosmological scales. The latter, referred to as MG theories, can create effective dark energy scenarios mimicking the behavior of actual dark energy. As a crucial avenue for explaining the acceleration, it is imperative to extend our investigation into MG models.

A prominent exemplar of such theoretical constructs is the DGP model [72]. It posits that gravity can leak from our four-dimensional Minkowski brane into an extra dimension of a five-dimensional bulk space-time. In this subsection, we constrain the DGP model and one of its phenomenological extensions.

1. Dvali-Gabadadze-Porrati model

In the DGP model, the Friedmann equation is modified as

$$3M_{\text{pl}}^2 \left(H^2 - \frac{H}{r_c} \right) = \rho_m (1+z)^3, \quad (26)$$

where $r_c = [H_0(1 - \Omega_m)]^{-1}$ is the length scale at which the phenomenon of gravitational leakage into the extra dimension occurs. Thus, the reduced Hubble parameter can be written as

$$E(z) = \sqrt{\Omega_m(1+z)^3 + \Omega_{r_c}} + \sqrt{\Omega_{r_c}}, \quad (27)$$

where $\Omega_{r_c} = (1 - \Omega_m)^2/4$.

From the joint constraints, we can get the best-fit parameters and the corresponding χ^2 :

$$\Omega_m = 0.245, \quad H_0 = 71.5 \text{ km/s/Mpc}, \quad \chi_{\text{min}}^2 = 1684.453.$$

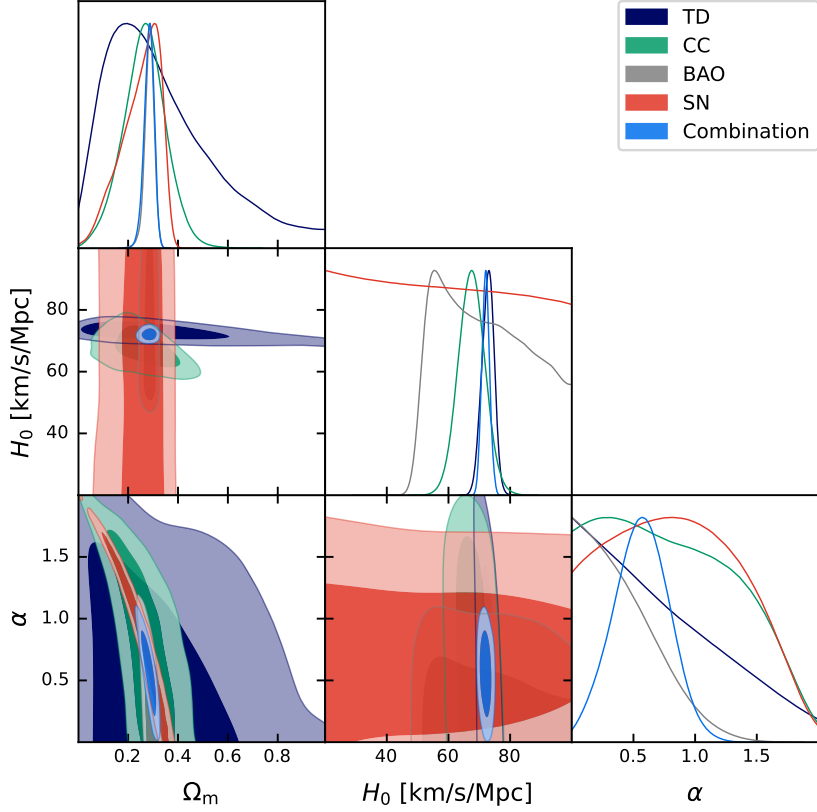


FIG. 12. The α DE model: 68.3% and 95.4% confidence contours derived from individual TD, CC, BAO, and SN datasets, and their combined analysis (TD+CC+BAO+SN).

We present the $1\sigma - 2\sigma$ posterior distribution contours for the DGP model in Fig. 11. As can be seen, the results tend toward a relatively low value of Ω_m , which is consistent with the findings reported in Ref. [107]. The DGP model shares an equivalent number of parameters with the flat Λ CDM model. Compared to flat Λ CDM, the DGP model yields a smaller χ_{\min}^2 , indicating a superior fit to the observational data. This model is the only one that is supported by both the AIC, BIC and DIC metrics, with $\Delta\text{AIC} = -1.829$, $\Delta\text{BIC} = -1.829$ and $\Delta\text{DIC} = -1.798$, though the magnitude of these values falls just below the threshold for positive evidence. It should be noted that this model is strongly disfavored when the CMB data are incorporated, as found in Refs. [74, 108–110].

2. α dark energy model

The α DE model emerges as a phenomenological extension of the DGP model, in which the Friedmann equation is modified as

$$3M_{\text{pl}}^2 \left(H^2 - \frac{H^\alpha}{r_c^{2-\alpha}} \right) = \rho_m(1+z)^3, \quad (28)$$

where α is a phenomenological parameter and $r_c = (1 - \Omega_m)^{1/(\alpha-2)} H_0^{-1}$. The reduced Hubble parameter can be

derived from the equation

$$E(z)^2 = \Omega_m(1+z)^3 + E(z)^\alpha(1 - \Omega_m). \quad (29)$$

It is evident that the α DE model transitions to the DGP model when the parameter α is set to 1, and it reduces to the Λ CDM model when α is taken as 0.

From the joint constraints, we obtain the best-fit parameters and the corresponding χ^2 :

$$\Omega_m = 0.284, \quad H_0 = 72.1 \text{ km/s/Mpc}, \quad \alpha = 0.56, \\ \chi_{\min}^2 = 1680.915.$$

We present the $1\sigma - 2\sigma$ posterior distribution contours for the α DE model in Fig. 12. As can be seen, the DGP ($\alpha = 1$) and Λ CDM ($\alpha = 0$) models are both ruled out by the current observational data at about 2σ confidence level. Compared to flat Λ CDM, the α DE model produces $\Delta\text{AIC} = -3.367$, $\Delta\text{DIC} = -3.547$ and $\Delta\text{BIC} = 2.175$. The AIC and DIC analyses indicate a preference for the α DE model (with positive evidence), whereas $\Delta\text{BIC} > 2$ suggests positive evidence against the α DE model.

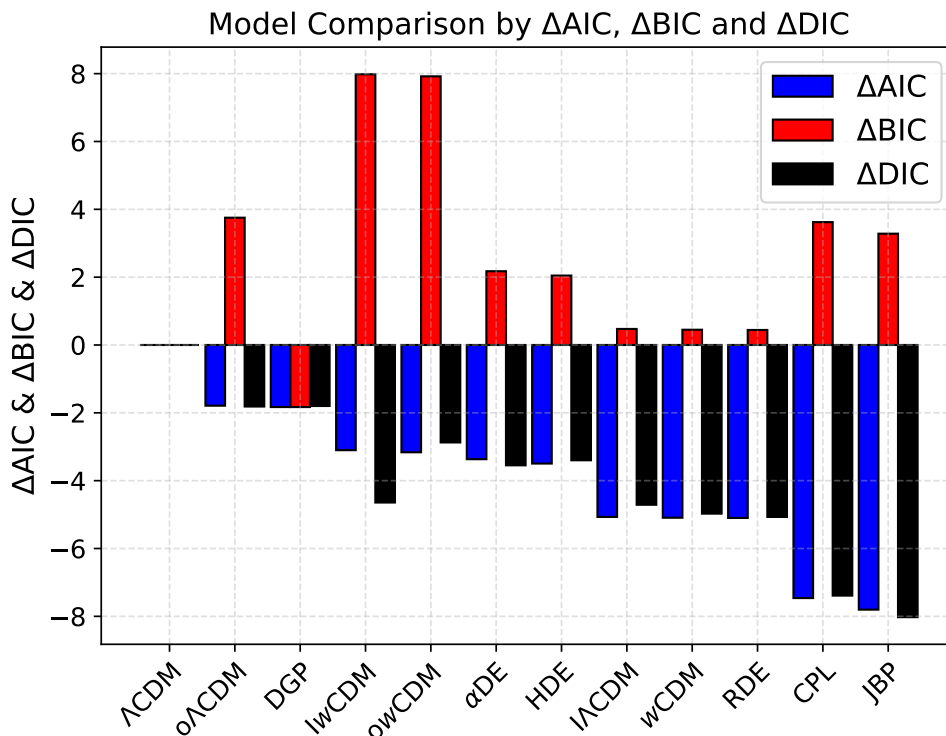


FIG. 13. Graphical representation of model comparison results. In this work, we choose flat Λ CDM as a reference model to calculate the Δ AIC, Δ BIC and Δ DIC values. Generally, a negative Δ A/B/DIC value within the range $[-2, 0)$ indicates weak evidence in favor of the model, a value within $[-6, -2)$ indicates positive evidence in favor, a value within $[-10, -6)$ indicates strong evidence in favor, and a value less than -10 indicates very strong evidence in favor. Conversely, a Δ A/B/DIC value within the range $(0, 2]$ indicates weak evidence against the model, a value within $(2, 6]$ indicates positive evidence against, a value within $(6, 10]$ indicates strong evidence against, and a value greater than 10 indicates very strong evidence against. The order of models from left to right is arranged according to the values of Δ AIC, i.e., in order of decreasing Δ AIC.

V. DISCUSSION AND CONCLUSION

The Λ CDM model remains the leading framework for dark energy due to its robust performance and consistent agreement with various observations. However, recent observations suggest that some competing dark energy models could potentially challenge its dominance. In this paper, we explore whether any of these models can match or even surpass the Λ CDM model in terms of fitting the current observational data. Given the discrepancies observed in measurements between the early- and late-time universe, our analysis is conducted using only the late-universe observations, including the baryon acoustic oscillation, type Ia supernova, cosmic chronometer, and strong gravitational lensing time delay data. The paper presents a thorough evaluation of twelve prominent cosmological models.

The dark energy models vary in their parameter count. Compared to the Λ CDM model, although these models can yield lower χ^2 values, this does not necessarily indicate superior performance. The reduced χ^2 values could be a consequence of overfitting, where models have captured the noise in data rather than the underlying patterns. Therefore, we employ AIC, BIC and DIC to

penalize the model complexity, thereby ensuring a fair assessment that balances goodness of fit with model simplicity. The model comparison results using the information criteria are summarized in Table V. To enhance visual comprehension, we present the numerical results in a graphical format in Fig. 13. We are only concerned with the relative values of AIC, BIC and DIC, rather than their absolute values. We calculate the Δ AIC, Δ BIC and Δ DIC values for each model, using the flat Λ CDM model as the reference.

From the perspective of AIC and DIC, all of the dark energy models perform better than the flat Λ CDM model. Generally, compared to the flat Λ CDM model, a model with $-2 \leq \Delta$ AIC, DIC < 0 is favored with weak evidence, $-6 \leq \Delta$ AIC, DIC < -2 indicates positive evidence in favor, $-10 \leq \Delta$ AIC, DIC < -6 indicates strong evidence in favor, and Δ AIC, DIC < -10 indicates very strong evidence in favor. All the dark energy models yield negative Δ AIC and Δ DIC values, indicating that although these models have been penalized by AIC and DIC for their increased complexity, they offer a better fit to the observational data. The dynamical dark energy models, specifically the CPL and JBP models, have demonstrated the best performance among all the cosmological models, and the constraint results indicate that

the cosmological constant scenario is excluded at the 3σ confidence level. From the results, we find compelling evidence forcing us away from the cosmological constant.

From the standpoint of BIC, the flat Λ CDM continues to exhibit excellent performance, with only one model being more favored. Typically, a BIC difference of 2 is generally indicative of significant evidence against the model with the higher BIC, while a difference within (2, 6] indicates positive evidence against, a value within (6, 10] indicates strong evidence against, and a value greater than 10 indicates very strong evidence against. Compared to the flat Λ CDM model, two models are strongly disfavored (Iw CDM, ow CDM; $6 < \Delta\text{BIC} \leq 10$), five models are significantly disfavored (CPL, JBP, $o\Lambda$ CDM, α DE, HDE; $2 < \Delta\text{BIC} \leq 6$), three models are weakly disfavored ($I\Lambda$ CDM, w CDM, RDE; $0 < \Delta\text{BIC} < 1$), and one model outperforms the Λ CDM model (DGP; $\Delta\text{BIC} = -1.829$). Overall, the BIC analysis leaves substantial room for the flat Λ CDM model.

Taking into account both the AIC, BIC and DIC analysis, only one model performs better than the flat Λ CDM model, i.e., DGP. The model outperforms all dark energy models, which implies that modified gravity theories, one of the two approaches to explaining the accelerated expansion of the universe, merit significant attention. In addition, the $I\Lambda$ CDM, w CDM, and RDE models are robust contenders to the Λ CDM model, all receiving substantial support from AIC and DIC, and not being significantly disapproved by BIC. Beyond these, all other models are supported by AIC and DIC (from weak to strong evidence) but disfavored by BIC (from positive to strong evidence). The divergent model selection preferences shown by AIC, BIC and DIC can be attributed to the lighter penalty of AIC and DIC on the number of model parameters, which tends to favor more complex models, while BIC imposes a heavier penalty on the model complexity, thus favoring simpler models.

We have detected numerous indications of new physics beyond the standard model, such as the possibility that the universe may be spatially open, dark energy may be dynamically evolving, there may be an interaction between dark matter and dark energy, all at high confidence levels. Additionally, we have explored the nature of dark energy from the perspective of quantum gravity, and this framework is well-received by the current observational data, especially the RDE model. It should be noted that some models cannot be effectively constrained. For instance, when exploring the spatial flatness of the universe or the interaction between dark sectors within the w CDM framework, we are unable to provide tight constraints. In cosmological research, considering multiple effects simultaneously is important due to the parameter degeneracy among these effects; however, the current data does not support such an approach. We can only hope for more data or the emergence of new probes to enable this [111].

In physics, the cosmic acceleration can be attributed to two primary mechanisms: either the presence of dark energy or modifications to the gravity on cosmological scales. In the present work, we primarily study dark energy models, while also considering two MG models, which we refer to as effective dark energy models that can mimic the behavior of dark energy. Surprisingly, the results indicate that one of the MG models, the DGP model, outperforms all the dark energy models we consider. In the forthcoming research, we plan to investigate a broader range of MG theories, exploring diverse modifications to gravity on large scales, to discern which scenarios are more favored by the current observational data.

ACKNOWLEDGMENTS

We thank Tian-Nuo Li and Guo-Hong Du for fruitful discussions.

-
- [1] N. Aghanim *et al.* (Planck), “Planck 2018 results. VI. Cosmological parameters,” *Astron. Astrophys.* **641**, A6 (2020), [arXiv:1807.06209 \[astro-ph.CO\]](#).
 - [2] Varun Sahni and Alexei A. Starobinsky, “The Case for a positive cosmological Lambda term,” *Int. J. Mod. Phys. D* **9**, 373–444 (2000), [arXiv:astro-ph/9904398](#).
 - [3] Chan-Gyung Park and Bharat Ratra, “Using the tilted flat- Λ CDM and the untilted non-flat Λ CDM inflation models to measure cosmological parameters from a compilation of observational data,” *Astrophys. J.* **882**, 158 (2019), [arXiv:1801.00213 \[astro-ph.CO\]](#).
 - [4] Alberto Domínguez, Radoslaw Wojtak, Justin Finke, Marco Ajello, Kari Helgason, Francisco Prada, Abhishek Desai, Vaidehi Paliya, Lea Marcotulli, and Dieter Hartmann, “A new measurement of the Hubble constant and matter content of the Universe using extragalactic background light γ -ray attenuation,” *Astrophys. J.* **885**, 137 (2019), [arXiv:1903.12097 \[astro-ph.CO\]](#).
 - [5] Chan-Gyung Park and Bharat Ratra, “Using SPT polarization, *Planck* 2015, and non-CMB data to constrain tilted spatially-flat and untilted nonflat Λ CDM, XCDM, and ϕ CDM dark energy inflation cosmologies,” *Phys. Rev. D* **101**, 083508 (2020), [arXiv:1908.08477 \[astro-ph.CO\]](#).
 - [6] Weikang Lin and Mustapha Ishak, “A Bayesian interpretation of inconsistency measures in cosmology,” *JCAP* **05**, 009 (2021), [arXiv:1909.10991 \[astro-ph.CO\]](#).
 - [7] Wendy L. Freedman, Barry F. Madore, Taylor Hoyt, In Sung Jang, Rachael Beaton, Myung Gyoon Lee, Andrew Monson, Jill Neeley, and Jeffrey Rich, “Calibration of the Tip of the Red Giant Branch (TRGB),” (2020), [10.3847/1538-4357/ab7339](#), [arXiv:2002.01550 \[astro-ph.GA\]](#).
 - [8] S. Birrer *et al.*, “TDCOSMO - IV. Hierarchical time-delay cosmography – joint inference of the Hubble con-

- stant and galaxy density profiles,” *Astron. Astrophys.* **643**, A165 (2020), [arXiv:2007.02941 \[astro-ph.CO\]](#).
- [9] G. Efstathiou, “A Lockdown Perspective on the Hubble Tension (with comments from the SH0ES team),” (2020), [arXiv:2007.10716 \[astro-ph.CO\]](#).
- [10] Supranta S. Boruah, Michael J. Hudson, and Guilhem Lavaux, “Peculiar velocities in the local Universe: comparison of different models and the implications for H0 and dark matter,” *Mon. Not. Roy. Astron. Soc.* **507**, 2697–2713 (2021), [arXiv:2010.01119 \[astro-ph.CO\]](#).
- [11] Wendy L. Freedman, “Measurements of the Hubble Constant: Tensions in Perspective,” *Astrophys. J.* **919**, 16 (2021), [arXiv:2106.15656 \[astro-ph.CO\]](#).
- [12] Qin Wu, Guo-Qiang Zhang, and Fa-Yin Wang, “An 8 per cent determination of the Hubble constant from localized fast radio bursts,” *Mon. Not. Roy. Astron. Soc.* **515**, L1–L5 (2022), [Erratum: *Mon. Not. Roy. Astron. Soc.* 531, L8 (2024)], [arXiv:2108.00581 \[astro-ph.CO\]](#).
- [13] Shulei Cao and Bharat Ratra, “Using lower redshift, non-CMB, data to constrain the Hubble constant and other cosmological parameters,” *Mon. Not. Roy. Astron. Soc.* **513**, 5686–5700 (2022), [arXiv:2203.10825 \[astro-ph.CO\]](#).
- [14] Yun Chen, Suresh Kumar, Bharat Ratra, and Tengpeng Xu, “Effects of Type Ia Supernovae Absolute Magnitude Priors on the Hubble Constant Value,” *Astrophys. J. Lett.* **964**, L4 (2024), [arXiv:2401.13187 \[astro-ph.CO\]](#).
- [15] Wendy L. Freedman, Barry F. Madore, Taylor J. Hoyt, In Sung Jang, Abigail J. Lee, and Kayla A. Owens, “Status Report on the Chicago-Carnegie Hubble Program (CCHP): Measurement of the Hubble Constant Using the Hubble and James Webb Space Telescopes,” *Astrophys. J.* **985**, 203 (2025), [arXiv:2408.06153 \[astro-ph.CO\]](#).
- [16] Simon Birrer *et al.* (TDCOSMO), “TDCOSMO 2025: Cosmological constraints from strong lensing time delays,” in *3rd General Meeting of CosmoVerse: Addressing observational tensions in cosmology with systematics and fundamental physics* (2025) [arXiv:2506.03023 \[astro-ph.CO\]](#).
- [17] George Efstathiou and Steven Gratton, “The evidence for a spatially flat Universe,” *Mon. Not. Roy. Astron. Soc.* **496**, L91–L95 (2020), [arXiv:2002.06892 \[astro-ph.CO\]](#).
- [18] Tonghua Liu, Shengjia Wang, Hengyu Wu, Shuo Cao, and Jieci Wang, “Newest Measurements of Cosmic Curvature with BOSS/eBOSS and DESI DR1 Baryon Acoustic Oscillation Observations,” *Astrophys. J. Lett.* **981**, L24 (2025), [arXiv:2411.14154 \[astro-ph.CO\]](#).
- [19] Javier de Cruz Perez, Chan-Gyung Park, and Bharat Ratra, “Updated observational constraints on spatially flat and nonflat Λ CDM and XCDM cosmological models,” *Phys. Rev. D* **110**, 023506 (2024), [arXiv:2404.19194 \[astro-ph.CO\]](#).
- [20] Jéferson A. S. Fortunato, Wiliam S. Hipólito-Ricaldi, and Gustavo E. Romero, “Probing Cosmic Curvature with Fast Radio Bursts and DESI DR2,” (2025), [arXiv:2506.01504 \[astro-ph.CO\]](#).
- [21] Angus H. Wright *et al.*, “KiDS-Legacy: Cosmological constraints from cosmic shear with the complete Kilo-Degree Survey,” (2025), [arXiv:2503.19441 \[astro-ph.CO\]](#).
- [22] Benjamin Stözlner *et al.*, “KiDS-Legacy: Consistency of cosmic shear measurements and joint cosmological constraints with external probes,” (2025), [arXiv:2503.19442 \[astro-ph.CO\]](#).
- [23] Frank J. Qu *et al.* (SPT-3G, ACT), “Unified and consistent structure growth measurements from joint ACT, SPT and Planck CMB lensing,” (2025), [arXiv:2504.20038 \[astro-ph.CO\]](#).
- [24] L. Verde, T. Treu, and A. G. Riess, “Tensions between the Early and the Late Universe,” *Nature Astron.* **3**, 891 (2019), [arXiv:1907.10625 \[astro-ph.CO\]](#).
- [25] Adam G. Riess *et al.*, “A Comprehensive Measurement of the Local Value of the Hubble Constant with 1 km s⁻¹ Mpc⁻¹ Uncertainty from the Hubble Space Telescope and the SH0ES Team,” *Astrophys. J. Lett.* **934**, L7 (2022), [arXiv:2112.04510 \[astro-ph.CO\]](#).
- [26] Sunny Vagnozzi, “Seven Hints That Early-Time New Physics Alone Is Not Sufficient to Solve the Hubble Tension,” *Universe* **9**, 393 (2023), [arXiv:2308.16628 \[astro-ph.CO\]](#).
- [27] Jun-Qian Jiang, Davide Pedrotti, Simony Santos da Costa, and Sunny Vagnozzi, “Nonparametric late-time expansion history reconstruction and implications for the Hubble tension in light of recent DESI and type Ia supernovae data,” *Phys. Rev. D* **110**, 123519 (2024), [arXiv:2408.02365 \[astro-ph.CO\]](#).
- [28] Sunny Vagnozzi, Eleonora Di Valentino, Stefano Gariazzo, Alessandro Melchiorri, Olga Mena, and Joseph Silk, “The galaxy power spectrum take on spatial curvature and cosmic concordance,” *Phys. Dark Univ.* **33**, 100851 (2021), [arXiv:2010.02230 \[astro-ph.CO\]](#).
- [29] Sunny Vagnozzi, Abraham Loeb, and Michele Moresco, “Eppur è piatto? The Cosmic Chronometers Take on Spatial Curvature and Cosmic Concordance,” *Astrophys. J.* **908**, 84 (2021), [arXiv:2011.11645 \[astro-ph.CO\]](#).
- [30] A. G. Adame *et al.* (DESI), “DESI 2024 VI: Cosmological Constraints from the Measurements of Baryon Acoustic Oscillations,” (2024), [arXiv:2404.03002 \[astro-ph.CO\]](#).
- [31] Peng-Ju Wu and Xin Zhang, “Measuring cosmic curvature with non-CMB observations,” (2024), [arXiv:2411.06356 \[astro-ph.CO\]](#).
- [32] P. J. E. Peebles and Bharat Ratra, “Cosmology with a Time Variable Cosmological Constant,” *Astrophys. J. Lett.* **325**, L17 (1988).
- [33] Bharat Ratra and P. J. E. Peebles, “Cosmological Consequences of a Rolling Homogeneous Scalar Field,” *Phys. Rev. D* **37**, 3406 (1988).
- [34] Ivaylo Zlatev, Li-Min Wang, and Paul J. Steinhardt, “Quintessence, cosmic coincidence, and the cosmological constant,” *Phys. Rev. Lett.* **82**, 896–899 (1999), [arXiv:astro-ph/9807002](#).
- [35] Paul J. Steinhardt, Li-Min Wang, and Ivaylo Zlatev, “Cosmological tracking solutions,” *Phys. Rev. D* **59**, 123504 (1999), [arXiv:astro-ph/9812313](#).
- [36] William J. Wolf, Pedro G. Ferreira, and Carlos García-García, “Matching current observational constraints with nonminimally coupled dark energy,” *Phys. Rev. D* **111**, L041303 (2025), [arXiv:2409.17019 \[astro-ph.CO\]](#).
- [37] Guillaume Payeur, Evan McDonough, and Robert Brandenberger, “Do Observations Prefer Thawing Quintessence?” (2024), [arXiv:2411.13637 \[astro-ph.CO\]](#).
- [38] William J. Wolf, Carlos García-García, Deaglan J.

- Bartlett, and Pedro G. Ferreira, “Scant evidence for thawing quintessence,” *Phys. Rev. D* **110**, 083528 (2024), [arXiv:2408.17318 \[astro-ph.CO\]](#).
- [39] Gen Ye, Matteo Martinelli, Bin Hu, and Alessandra Silvestri, “Non-minimally coupled gravity as a physically viable fit to DESI 2024 BAO,” (2024), [arXiv:2407.15832 \[astro-ph.CO\]](#).
- [40] Luis A. Escamilla, William Giarè, Eleonora Di Valentino, Rafael C. Nunes, and Sunny Vagnozzi, “The state of the dark energy equation of state circa 2023,” *JCAP* **05**, 091 (2024), [arXiv:2307.14802 \[astro-ph.CO\]](#).
- [41] Michel Chevallier and David Polarski, “Accelerating universes with scaling dark matter,” *Int. J. Mod. Phys. D* **10**, 213–224 (2001), [arXiv:gr-qc/0009008](#).
- [42] Eric V. Linder, “Exploring the expansion history of the universe,” *Phys. Rev. Lett.* **90**, 091301 (2003), [arXiv:astro-ph/0208512](#).
- [43] Christof Wetterich, “Phenomenological parameterization of quintessence,” *Phys. Lett. B* **594**, 17–22 (2004), [arXiv:astro-ph/0403289](#).
- [44] Eric V. Linder, “The paths of quintessence,” *Phys. Rev. D* **73**, 063010 (2006), [arXiv:astro-ph/0601052](#).
- [45] H. K. Jassal, J. S. Bagla, and T. Padmanabhan, “WMAP constraints on low redshift evolution of dark energy,” *Mon. Not. Roy. Astron. Soc.* **356**, L11–L16 (2005), [arXiv:astro-ph/0404378](#).
- [46] Jing-Zhe Ma and Xin Zhang, “Probing the dynamics of dark energy with novel parametrizations,” *Phys. Lett. B* **699**, 233–238 (2011), [arXiv:1102.2671 \[astro-ph.CO\]](#).
- [47] Kazuharu Bamba, Salvatore Capozziello, Shin’ichi Nojiri, and Sergei D. Odintsov, “Dark energy cosmology: the equivalent description via different theoretical models and cosmography tests,” *Astrophys. Space Sci.* **342**, 155–228 (2012), [arXiv:1205.3421 \[gr-qc\]](#).
- [48] Will Handley, “Curvature tension: evidence for a closed universe,” *Phys. Rev. D* **103**, L041301 (2021), [arXiv:1908.09139 \[astro-ph.CO\]](#).
- [49] Eleonora Di Valentino, Alessandro Melchiorri, and Joseph Silk, “Planck evidence for a closed Universe and a possible crisis for cosmology,” *Nature Astron.* **4**, 196–203 (2019), [arXiv:1911.02087 \[astro-ph.CO\]](#).
- [50] Jussi Valiviita, Elisabetta Majerotto, and Roy Maartens, “Instability in interacting dark energy and dark matter fluids,” *JCAP* **07**, 020 (2008), [arXiv:0804.0232 \[astro-ph\]](#).
- [51] Kazuya Koyama, Roy Maartens, and Yong-Seon Song, “Velocities as a probe of dark sector interactions,” *JCAP* **10**, 017 (2009), [arXiv:0907.2126 \[astro-ph.CO\]](#).
- [52] Timothy Clemson, Kazuya Koyama, Gong-Bo Zhao, Roy Maartens, and Jussi Valiviita, “Interacting Dark Energy – constraints and degeneracies,” *Phys. Rev. D* **85**, 043007 (2012), [arXiv:1109.6234 \[astro-ph.CO\]](#).
- [53] Yun-He Li, Jing-Fei Zhang, and Xin Zhang, “Parametrized Post-Friedmann Framework for Interacting Dark Energy,” *Phys. Rev. D* **90**, 063005 (2014), [arXiv:1404.5220 \[astro-ph.CO\]](#).
- [54] Yun-He Li and Xin Zhang, “Large-scale stable interacting dark energy model: Cosmological perturbations and observational constraints,” *Phys. Rev. D* **89**, 083009 (2014), [arXiv:1312.6328 \[astro-ph.CO\]](#).
- [55] Dong-Mei Xia and Sai Wang, “Constraining interacting dark energy models with latest cosmological observations,” *Mon. Not. Roy. Astron. Soc.* **463**, 952–956 (2016), [arXiv:1608.04545 \[astro-ph.CO\]](#).
- [56] Eleonora Di Valentino, Alessandro Melchiorri, Olga Mena, and Sunny Vagnozzi, “Interacting dark energy in the early 2020s: A promising solution to the H_0 and cosmic shear tensions,” *Phys. Dark Univ.* **30**, 100666 (2020), [arXiv:1908.04281 \[astro-ph.CO\]](#).
- [57] Eleonora Di Valentino, Alessandro Melchiorri, Olga Mena, and Sunny Vagnozzi, “Nonminimal dark sector physics and cosmological tensions,” *Phys. Rev. D* **101**, 063502 (2020), [arXiv:1910.09853 \[astro-ph.CO\]](#).
- [58] William Giarè, Miguel A. Sabogal, Rafael C. Nunes, and Eleonora Di Valentino, “Interacting Dark Energy after DESI Baryon Acoustic Oscillation Measurements,” *Phys. Rev. Lett.* **133**, 251003 (2024), [arXiv:2404.15232 \[astro-ph.CO\]](#).
- [59] Tian-Nuo Li, Peng-Ju Wu, Guo-Hong Du, Shang-Jie Jin, Hai-Li Li, Jing-Fei Zhang, and Xin Zhang, “Constraints on Interacting Dark Energy Models from the DESI Baryon Acoustic Oscillation and DES Supernovae Data,” *Astrophys. J.* **976**, 1 (2024), [arXiv:2407.14934 \[astro-ph.CO\]](#).
- [60] Emanuely Silva, Miguel A. Sabogal, Mateus S. Souza, Rafael C. Nunes, Eleonora Di Valentino, and Suresh Kumar, “New Constraints on Interacting Dark Energy from DESI DR2 BAO Observations,” (2025), [arXiv:2503.23225 \[astro-ph.CO\]](#).
- [61] Supriya Pan, Sivasish Paul, Emmanuel N. Saridakis, and Weiqiang Yang, “Interacting dark energy after DESI DR2: a challenge for Λ CDM paradigm?” (2025), [arXiv:2504.00994 \[astro-ph.CO\]](#).
- [62] Tian-Nuo Li, Guo-Hong Du, Yun-He Li, Peng-Ju Wu, Shang-Jie Jin, Jing-Fei Zhang, and Xin Zhang, “Probing the sign-changeable interaction between dark energy and dark matter with DESI baryon acoustic oscillations and DES supernovae data,” (2025), [arXiv:2501.07361 \[astro-ph.CO\]](#).
- [63] Andrew G. Cohen, David B. Kaplan, and Ann E. Nelson, “Effective field theory, black holes, and the cosmological constant,” *Phys. Rev. Lett.* **82**, 4971–4974 (1999), [arXiv:hep-th/9803132](#).
- [64] Miao Li, “A Model of holographic dark energy,” *Phys. Lett. B* **603**, 1 (2004), [arXiv:hep-th/0403127](#).
- [65] Changjun Gao, Fengquan Wu, Xuelei Chen, and You-Gen Shen, “A Holographic Dark Energy Model from Ricci Scalar Curvature,” *Phys. Rev. D* **79**, 043511 (2009), [arXiv:0712.1394 \[astro-ph\]](#).
- [66] Tian-Nuo Li, Yun-He Li, Guo-Hong Du, Peng-Ju Wu, Lu Feng, Jing-Fei Zhang, and Xin Zhang, “Revisiting holographic dark energy after DESI 2024,” (2024), [arXiv:2411.08639 \[astro-ph.CO\]](#).
- [67] Jun-Xian Li and Shuang Wang, “A comprehensive numerical study on four categories of holographic dark energy models,” (2024), [arXiv:2412.09064 \[astro-ph.CO\]](#).
- [68] Xin Tang, Yin-Zhe Ma, Wei-Ming Dai, and Hong-Jian He, “Constraining holographic dark energy and analyzing cosmological tensions,” *Phys. Dark Univ.* **46**, 101568 (2024), [arXiv:2407.08427 \[astro-ph.CO\]](#).
- [69] Oem Trivedi and Robert J. Scherrer, “New perspectives on future rip scenarios with holographic dark energy,” *Phys. Rev. D* **110**, 023521 (2024), [arXiv:2404.08912 \[astro-ph.CO\]](#).
- [70] H. Moradpour, A. H. Ziaie, and M. Kord Zangeneh, “Generalized entropies and corresponding holographic dark energy models,” *Eur. Phys. J. C* **80**, 732 (2020),

- arXiv:2005.06271 [gr-qc].
- [71] Tanay Kibe, Prabha Mandayam, and Ayan Mukhopadhyay, “Holographic spacetime, black holes and quantum error correcting codes: a review,” *Eur. Phys. J. C* **82**, 463 (2022), arXiv:2110.14669 [hep-th].
- [72] G. R. Dvali, Gregory Gabadadze, and Massimo Porrati, “4-D gravity on a brane in 5-D Minkowski space,” *Phys. Lett. B* **485**, 208–214 (2000), arXiv:hep-th/0005016.
- [73] Gia Dvali and Michael S. Turner, “Dark Energy as a Modification of the Friedmann Equation,” (2003), arXiv:astro-ph/0301510.
- [74] Yue-Yao Xu and Xin Zhang, “Comparison of dark energy models after Planck 2015,” *Eur. Phys. J. C* **76**, 588 (2016), arXiv:1607.06262 [astro-ph.CO].
- [75] A. G. Adame *et al.* (DESI), “DESI 2024 III: Baryon Acoustic Oscillations from Galaxies and Quasars,” (2024), arXiv:2404.03000 [astro-ph.CO].
- [76] A. G. Adame *et al.* (DESI), “DESI 2024 IV: Baryon Acoustic Oscillations from the Lyman Alpha Forest,” (2024), arXiv:2404.03001 [astro-ph.CO].
- [77] K. Lodha *et al.* (DESI), “Extended Dark Energy analysis using DESI DR2 BAO measurements,” (2025), arXiv:2503.14743 [astro-ph.CO].
- [78] T. M. C. Abbott *et al.* (DES), “The Dark Energy Survey: Cosmology Results With ~ 1500 New High-redshift Type Ia Supernovae Using The Full 5-year Dataset,” (2024), arXiv:2401.02929 [astro-ph.CO].
- [79] Michele Moresco *et al.*, “Unveiling the Universe with emerging cosmological probes,” *Living Rev. Rel.* **25**, 6 (2022), arXiv:2201.07241 [astro-ph.CO].
- [80] S. H. Suyu, P. J. Marshall, M. W. Auger, S. Hilbert, R. D. Blandford, L. V. E. Koopmans, C. D. Fassnacht, and T. Treu, “Dissecting the Gravitational Lens B1608+656. II. Precision Measurements of the Hubble Constant, Spatial Curvature, and the Dark Energy Equation of State,” *Astrophys. J.* **711**, 201–221 (2010), arXiv:0910.2773 [astro-ph.CO].
- [81] Inh Jee, Sherry Suyu, Eiichiro Komatsu, Christopher D. Fassnacht, Stefan Hilbert, and Léon V. E. Koopmans, “A measurement of the Hubble constant from angular diameter distances to two gravitational lenses,” (2019), 10.1126/science.aat7371, arXiv:1909.06712 [astro-ph.CO].
- [82] S. H. Suyu *et al.*, “Cosmology from gravitational lens time delays and Planck data,” *Astrophys. J. Lett.* **788**, L35 (2014), arXiv:1306.4732 [astro-ph.CO].
- [83] Geoff C. F. Chen *et al.*, “A SHARP view of H0LiCOW: H_0 from three time-delay gravitational lens systems with adaptive optics imaging,” *Mon. Not. Roy. Astron. Soc.* **490**, 1743–1773 (2019), arXiv:1907.02533 [astro-ph.CO].
- [84] Kenneth C. Wong *et al.*, “H0LiCOW – IV. Lens mass model of HE 0435–1223 and blind measurement of its time-delay distance for cosmology,” *Mon. Not. Roy. Astron. Soc.* **465**, 4895–4913 (2017), arXiv:1607.01403 [astro-ph.CO].
- [85] S. Birrer *et al.*, “H0LiCOW - IX. Cosmographic analysis of the doubly imaged quasar SDSS 1206+4332 and a new measurement of the Hubble constant,” *Mon. Not. Roy. Astron. Soc.* **484**, 4726 (2019), arXiv:1809.01274 [astro-ph.CO].
- [86] Cristian E. Rusu *et al.*, “H0LiCOW XII. Lens mass model of WFI2033 – 4723 and blind measurement of its time-delay distance and H_0 ,” *Mon. Not. Roy. Astron. Soc.* **498**, 1440–1468 (2020), arXiv:1905.09338 [astro-ph.CO].
- [87] A. J. Shajib *et al.* (DES), “STRIDES: a 3.9 per cent measurement of the Hubble constant from the strong lens system DES J0408–5354,” *Mon. Not. Roy. Astron. Soc.* **494**, 6072–6102 (2020), arXiv:1910.06306 [astro-ph.CO].
- [88] A. Agnello *et al.*, “Models of the strongly lensed quasar DES J0408–5354,” *Mon. Not. Roy. Astron. Soc.* **472**, 4038–4050 (2017), arXiv:1702.00406 [astro-ph.GA].
- [89] David W. Hogg, “Distance measures in cosmology,” (1999), arXiv:astro-ph/9905116.
- [90] Cong Zhang, Han Zhang, Shuo Yuan, Tong-Jie Zhang, and Yan-Chun Sun, “Four new observational $H(z)$ data from luminous red galaxies in the Sloan Digital Sky Survey data release seven,” *Res. Astron. Astrophys.* **14**, 1221–1233 (2014), arXiv:1207.4541 [astro-ph.CO].
- [91] Joan Simon, Licia Verde, and Raul Jimenez, “Constraints on the redshift dependence of the dark energy potential,” *Phys. Rev. D* **71**, 123001 (2005), arXiv:astro-ph/0412269.
- [92] M. Moresco *et al.*, “Improved constraints on the expansion rate of the Universe up to $z \sim 1.1$ from the spectroscopic evolution of cosmic chronometers,” *JCAP* **08**, 006 (2012), arXiv:1201.3609 [astro-ph.CO].
- [93] Michele Moresco, Lucia Pozzetti, Andrea Cimatti, Raul Jimenez, Claudia Maraston, Licia Verde, Daniel Thomas, Annalisa Citro, Rita Tojeiro, and David Wilkinson, “A 6% measurement of the Hubble parameter at $z \sim 0.45$: direct evidence of the epoch of cosmic re-acceleration,” *JCAP* **05**, 014 (2016), arXiv:1601.01701 [astro-ph.CO].
- [94] A. L. Ratsimbazafy, S. I. Loubser, S. M. Crawford, C. M. Cress, B. A. Bassett, R. C. Nichol, and P. Väisänen, “Age-dating Luminous Red Galaxies observed with the Southern African Large Telescope,” *Mon. Not. Roy. Astron. Soc.* **467**, 3239–3254 (2017), arXiv:1702.00418 [astro-ph.CO].
- [95] Daniel Stern, Raul Jimenez, Licia Verde, Marc Kamionkowski, and S. Adam Stanford, “Cosmic Chronometers: Constraining the Equation of State of Dark Energy. I: $H(z)$ Measurements,” *JCAP* **02**, 008 (2010), arXiv:0907.3149 [astro-ph.CO].
- [96] Nicola Borghi, Michele Moresco, and Andrea Cimatti, “Toward a Better Understanding of Cosmic Chronometers: A New Measurement of $H(z)$ at $z \sim 0.7$,” *Astrophys. J. Lett.* **928**, L4 (2022), arXiv:2110.04304 [astro-ph.CO].
- [97] Michele Moresco, “Raising the bar: new constraints on the Hubble parameter with cosmic chronometers at $z \sim 2$,” *Mon. Not. Roy. Astron. Soc.* **450**, L16–L20 (2015), arXiv:1503.01116 [astro-ph.CO].
- [98] William Giarè, Mahdi Najafi, Supriya Pan, Eleonora Di Valentino, and Javad T. Firouzjaee, “Robust preference for Dynamical Dark Energy in DESI BAO and SN measurements,” *JCAP* **10**, 035 (2024), arXiv:2407.16689 [astro-ph.CO].
- [99] William J. Wolf, Carlos García-García, and Pedro G. Ferreira, “Robustness of dark energy phenomenology across different parameterizations,” (2025), arXiv:2502.04929 [astro-ph.CO].
- [100] William J. Wolf, Carlos García-García, Theodore Anton, and Pedro G. Ferreira, “The Cosmological Evidence for Non-Minimal Coupling,” (2025),

- arXiv:2504.07679 [astro-ph.CO].
- [101] Andronikos Paliathanasis, “Observational Constraints on Dark Energy Models with Λ as an Equilibrium Point,” (2025), arXiv:2502.16221 [astro-ph.CO].
- [102] Andronikos Paliathanasis, “Dark Energy within the Generalized Uncertainty Principle in Light of DESI DR2,” (2025), arXiv:2503.20896 [astro-ph.CO].
- [103] Chan-Gyung Park, Javier de Cruz Pérez, and Bharat Ratra, “Using non-DESI data to confirm and strengthen the DESI 2024 spatially flat w_0w_a CDM cosmological parametrization result,” *Phys. Rev. D* **110**, 123533 (2024), arXiv:2405.00502 [astro-ph.CO].
- [104] Chan-Gyung Park, Javier de Cruz Pérez, and Bharat Ratra, “Is the w_0w_a CDM cosmological parameterization evidence for dark energy dynamics partially caused by the excess smoothing of Planck CMB anisotropy data?” (2024), arXiv:2410.13627 [astro-ph.CO].
- [105] G. Bargiacchi, M. Benetti, S. Capozziello, E. Lusso, G. Risaliti, and M. Signorini, “Quasar cosmology: dark energy evolution and spatial curvature,” *Mon. Not. Roy. Astron. Soc.* **515**, 1795–1806 (2022), arXiv:2111.02420 [astro-ph.CO].
- [106] Denitsa Staicova, “DE Models with Combined $H_0 \cdot r_d$ from BAO and CMB Dataset and Friends,” *Universe* **8**, 631 (2022), arXiv:2211.08139 [astro-ph.CO].
- [107] R. Camilleri *et al.* (DES), “The dark energy survey supernova program: investigating beyond- Λ CDM,” *Mon. Not. Roy. Astron. Soc.* **533**, 2615–2639 (2024), arXiv:2406.05048 [astro-ph.CO].
- [108] Zhongxu Zhai, Michael Blanton, Anže Slosar, and Jeremy Tinker, “An Evaluation of Cosmological Models from the Expansion and Growth of Structure Measurements,” *Astrophys. J.* **850**, 183 (2017), arXiv:1705.10031 [astro-ph.CO].
- [109] Zhengxiang Li, Puxun Wu, and Hongwei Yu, “Testing nonstandard cosmological models with SNLS3 supernova data and other cosmological probes,” *Astrophys. J.* **744**, 176 (2012), arXiv:1109.6125 [astro-ph.CO].
- [110] Lucas Lombriser, Wayne Hu, Wenjuan Fang, and Uros Seljak, “Cosmological Constraints on DGP Braneworld Gravity with Brane Tension,” *Phys. Rev. D* **80**, 063536 (2009), arXiv:0905.1112 [astro-ph.CO].
- [111] Peng-Ju Wu, Yue Shao, Shang-Jie Jin, and Xin Zhang, “A path to precision cosmology: synergy between four promising late-universe cosmological probes,” *JCAP* **06**, 052 (2023), arXiv:2202.09726 [astro-ph.CO].